European Journal of Medicinal Chemistry 284 (2025) 117176

Contents lists available at ScienceDirect

European Journal of Medicinal Chemistry

journal homepage: www.elsevier.com/locate/ejmech

Research paper

# Correction of aberrant splicing of ELP1 pre-mRNA by kinetin derivatives – A structure activity relationship study

Barbara Maková [a,1], Václav Mik [a,1], Barbora Lišková [b], Lenka Drašarová [c], Martina Medvedíková [b], Alena Hořínková [a], Petr Vojta [b,f], Marek Zatloukal [d], Lucie Plíhalová [d], Martin Hönig [d], Karel Doležal [d,e], Kristýna Forejt [a], Tomáš Oždian [b], Marián Hajdúch [b], Miroslav Strnad [e], Jiří Voller [a,b,*]

[a] Laboratory of Experimental Biology, Faculty of Science, Palacký University, Šlechtitelů 27, CZ-78371 Olomouc, Czech Republic
[b] Institute of Molecular and Translational Medicine, Faculty of Medicine and Dentistry, Palacký University, Hněvotínská 3, 775 15 Olomouc, Czech Republic
[c] Isotope Laboratory, Institute of Experimental Botany, Academy of Sciences of the Czech Republic, Vídeňská 1083, 142 00 Prague 4, Czech Republic
[d] Department of Chemical Biology, Faculty of Science, Palacký University, Šlechtitelů 27, CZ-78371 Olomouc, Czech Republic
[e] Laboratory of Growth Regulators, Institute of Experimental Botany AS CR & Palacký University, Šlechtitelů 27, CZ-78371 Olomouc, Czech Republic
[f] University of Natural Resources and Life Sciences, Vienna, Department of Biotechnology, Institute of Computational Biology, Vienna, Austria

ARTICLE INFO

*Keywords:*
Kinetin
Cytokinin
ELP1
Alternative splicing
mRNA metabolism
ADME *in vitro*

ABSTRACT

Familial dysautonomia is a debilitating congenital neurodegenerative disorder with no causative therapy. It is caused by a homozygous mutation in ELP1 gene, resulting in the production of the transcript lacking exon 20. The compounds studied as potential treatments include the clinical candidate kinetin, a plant hormone from the cytokinin family. We explored the relationship between the structure of a set of kinetin derivatives (N = 72) and their ability to correct aberrant splicing of the ELP1 gene. Active compounds can be obtained by the substitution of the purine ring with chlorine and fluorine at the C2 atom, with a small alkyl group at the N7 atom, or with diverse groups at the C8 atom. On the other hand, a substitution at the N3 or N9 atoms resulted in a loss of activity. We successfully tested a hypothesis inspired by the remarkable tolerance of the position C8 to substitution, postulating that the imidazole of the purine moiety is not required for the activity. We also evaluated the activity of phytohormones from other families, but none of them corrected ELP1 mRNA aberrant splicing. A panel of *in vitro* ADME assays, including evaluation of transport across model barriers, stability in plasma and in the presence of liver microsomal fraction as well as plasma protein binding, was used for an initial estimation of the potential bioavailability of the active compounds. Finally, a RNA-seq data suggest that 8-aminokinetin modulates expression spliceosome components.

## 1. Introduction

Familial dysautonomia (FD) (Riley-Day syndrome, hereditary sensory and autonomic neuropathy type III, OMIM number #223900) [73] is a debilitating congenital neurodegeneration with no causative therapy. It affects the development and survival of neurons of both sensory and autonomic nervous systems [26,73]. The symptoms include the abnormal perception of pain and heat, inability to produce tears and also problems with speech and swallowing [27,49,73,82]. Patients have labile blood pressure, gastrointestinal dysfunction and vomiting crises. Pneumonia resulting from misdirected swallowing or the aspiration of stomach contents during vomiting crises is the leading cause of death [27,28]. Motoric ability is affected (incoordination, unsteady gait), intelligence is not. Somatic growth is slowed down and life expectancy is decreased; [1,25,74,77]).

The disease has the highest prevalence among persons of Ashkenazi Jewish descent [26]. In over 99 % of the cases, the disease is caused by a recessive point mutation in the donor splice site of intron 20 (IVS20+6T→C) of ELP1 gene (formerly known as IKAP, IkB kinase-associated protein) [20,80]. The mutation results in the reduced splicing efficiency, whereby the exon 20 is skipped and the truncated form of ELP1 protein is expressed. The incomplete penetrance of the mutation allows for the production of the lower amount of the wild-type

* Corresponding author. Laboratory of Experimental Biology, Faculty of Science, Palacký University, Šlechtitelů 27, CZ-78371 Olomouc, Czech Republic.
*E-mail address:* jiri.voller@upol.cz (J. Voller).
[1] Contributed equally to the study.

https://doi.org/10.1016/j.ejmech.2024.117176
Received 6 July 2024; Received in revised form 14 December 2024; Accepted 15 December 2024
Available online 17 December 2024

**List of abbreviations:**

| | |
|---|---|
| ADME | absorption – distribution – metabolism – excretion |
| BBB | blood-brain barrier |
| Boc | tert-butoxycarbonyl group |
| DIAD | diisopropyl azodicarboxylate |
| DMF | dimethyl formamide |
| DMSO | dimethyl sulfoxide |
| EGCG | epigallocatechin gallate |
| ELP1 | elongator complex protein 1 |
| FD | familial dysautonomia |
| GO | Gene Ontology |
| HBBS | Hank's balanced buffer solution |
| LDA | lithium diisopropylamide |
| MDCK | Madin-Darby Canine Kidney cells |
| MDR1 | multidrug resistance 1 |
| PAMPA | parallel artificial membrane permeability assay |
| PBS | phosphate buffer saline |
| RED | rapid equilibrium dialysis |
| THF | tetrahydrofuran |
| THP | tetrahydropyran |

transcript and functional protein. The effect is tissue-specific. Neurons, in contrast to, for example, peripheral lymphocytes, produce the aberrant transcript predominantly [41,80].

Although the pathology of the disease is not fully understood, the recent advances in models of FD including neurons generated from embryonic or induced pluripotent stem cells [60–62,86,93] and humanized FD mouse [30,50,66,67] allowed important insights into both the molecular and developmental consequences of the ELP1 gene mutation. Loss of ELP1 function in a mouse model [36] led to abnormal behaviour of nervous system progenitors, neuronal stress and apoptosis as well as to decrease in retrograde transport of nerve growth factor. All these processes contribute to the abnormal innervation of target structures.

The ELP1 protein is a scaffolding subunit of the conserved Elongator complex, but it also has independent functions. The Elongator complex regulates polymerase II transcriptional activity [46] and histone acetylation [57]. The Elongator plays a role in many processes related to development and functions of the nervous system such as cell motility [38], actin cytoskeleton organization [54], tubulin phosphorylation intracellular trafficking [40], exocytosis and polarized secretion [72]. Expression studies showed that the canonical ELP1 mutation results in dysregulation of genes involved in oligodendrocyte differentiation and/or myelin formation in patients' cerebrum tissue [37], genes related to peripheral neurogenesis and neuronal differentiation in IPS-derived neural crest precursors [60] and synaptic vesicular and neuronal transport genes in embryonic stem cell-derived peripheral neural system neurons [62].

The current therapy of FD is symptomatic [70]. However, the neuronal dysfunction and the progressive loss of neurons throughout the life suggest that FD patients of all ages could benefit from a pharmacological correction of the aberrant ELP1 pre-mRNA splicing. Experimental approaches include delivery of therapeutic nucleic acids (antisense oligonucleotides [44] and exon-specific U1 snRNAs [79], as well as treatment with small molecules. Phosphatidylserine protects affected neurons [56] by decreasing histone deacetylase levels and thus increasing acetylation of α-tubulin [68]. Other compounds induce expression of wild-type ELP1 protein. Treatment of patient fibroblasts with polyphenol (−)-epigallocatechin gallate (EGCG) increases the inclusion of exon 20 [22,23]. Other compounds increasing exon 20 inclusion were reported: isoflavones genistein and daidzein [21], cardiac glycosides [63] and proteasome inhibitor carfilzomib [48].

Slaugenhaupt *et al.* [81] discovered that kinetin ($N^6$-furfuryladenine) and $N^6$-benzyladenine, plant hormones from the cytokinin family with diverse effects in human cells (reviewed in [55,87], decrease the skipping of exon 20 by the splicing machinery. Orally administered kinetin corrected the splicing defect in the tissues including the brain of the mouse expressing mutant human ELP1 gene [3]. Also, an initial trial in patients yielded promising results - kinetin increased the levels of the wild-type transcript in peripheral blood leukocytes and was well tolerated [29]. Later discovered a more potent kinetin derivative (2-chlorokinetin) and named it RECTAS [91]. In a follow-up paper, it was reported that RECTAS interacts with CDC-like kinases (CLKs) and enhances the phosphorylation of SRSF6 [2]. Similar to kinetin, RECTAS has only a limited effect on transcription and overall splicing [2,3], which may reduce the side effects of therapy. Recently Salani *et al.* [75] developed a cell-based luciferase splicing assay for high-throughput quantification of the ELP1 exon 20 inclusion and used it to screen cytokinin derivatives. However, they reveal structures of only two active compounds, namely 2-chloro-8-[(3,3-difluorocyclobutyl)methoxy]-*N*-(thiazol-2-ylmethyl)-9*H*-purin-6-amine and 2-chloro-8-(2-methoxyethoxy)-*N*-(pyrimidin-4-ylmethyl)-9*H*-purin-6-amine. In both compounds, the furan ring is replaced by another aromatic ring. A recently granted patent by Slaugenhaupt *et al.* [4] revealed a large set of $N^6$-substituted adenines, including $N^6$-furfurylamino derivatives that modulate ELP1 splicing. The majority of the compounds claimed in the patent have 2-chloro substitutions, and several purine bioisosteres are also disclosed. Additionally, a systematic study of purine isosteres of kinetin was conducted by Maková *et al.* [5].

However, to date, no systematic peer reviewed structure-activity relationship study of kinetin substitution derivatives has been published.

In this study, we explored the relationship between the structure of a large set of kinetin derivatives (N = 72) and evaluated their ability to correct aberrant splicing of ELP1 gene due to a missense mutation in the donor splice site. We also tested the hypothesis that kinetin analogues without the imidazole ring and other classes of phytohormones have this activity. A panel of *in vitro* ADME assays was used to evaluate the potential bioavailability of the active compounds. Finally, we used transcriptomic profiling to study mechanism of action of one of the active derivatives.

## 2. Results

### 2.1. Synthesis

A group of C2 substituted kinetin derivatives was prepared, generally in moderate to excellent yields, either by nucleophilic substitution of chlorine at the *C*6 atom of readily available purine building blocks by furfurylamine and $Et_3N$ in refluxing *n*PrOH (**2-5**) or by the reaction of **2** with large excess of corresponding nucleophile agent under elevated temperature (**6-9**) (Fig. 1).

Methyl group was introduced to the N3 atom of kinetin by the reaction of **1** with MeI in dry DMA using similar reaction conditions as published by Mik *et al.* [65] (Fig. 2). The reaction provided **10** as a main product, while the minor N9 isomer was easily removed by column chromatography. However, the $^1H$ and $^{13}C$ NMR spectra of **10** clearly showed presence of two sets of signals, further NMR experiments confirmed existence of **10** in two tautomeric forms in a molar ratio approximately 2.5:1.

N7 kinetin derivatives were prepared in two steps (Fig. 3). Firstly, 7-substituted 6-chloro/2,6-dichloropurine intermediates (**Ia-IVa**) were isolated as minor products during alkylation of 6-chloro/2,6-dichloropurine in DMF and in the presence of $K_2CO_3$ in 16–20 % yield. Further, **Ia-IVa** were allowed to react with furfurylamine and $Et_3N$ in refluxing *n*PrOH for 4 h to give desired products **11-14** in 43–76 % yield.

The majority of C8 substituted kinetin derivatives were synthesized following previously described protocol [17]. Shortly, heating of 9-THP protected 6-chloropurine **V** [85] with furfurylamine and $Et_3N$ in *n*PrOH

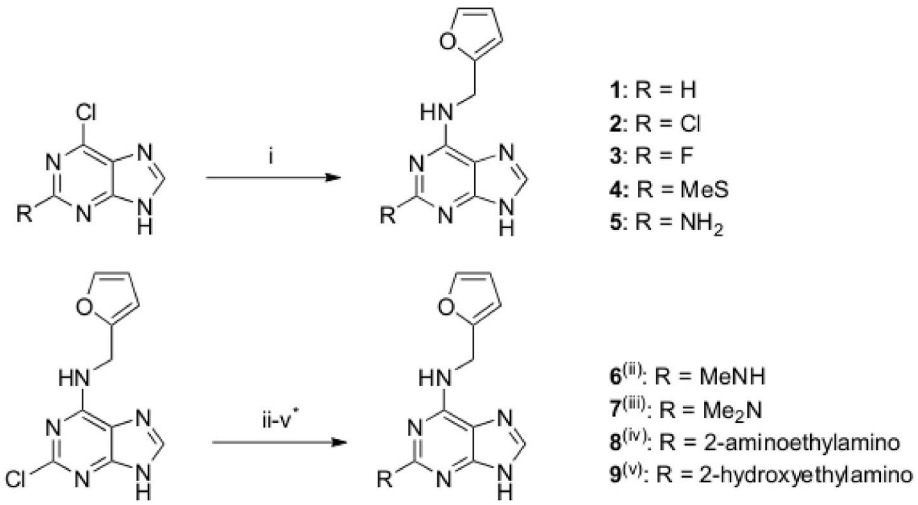


**Fig. 1.** Reagents and conditions: i) furfurylamine, $Et_3N$, nPrOH or nBuOH (for 4), 100 °C, 4 or 12 h (for 4), 93 % (for 2), 40 % (for 3), 60 % (for 4), 48 % (for 5); ii) 8 M $MeNH_2$ in EtOH, 95 °C, overnight, 69 %; iii) 5.6 M $Me_2NH$ in EtOH, 100 °C, 17 h, 93 %; iv) ethane-1,2-diamine, 165 °C, 3 h, 76 %; v) 2-aminoethanol, 165 °C, 3 h, 75 %; * - various conditions.

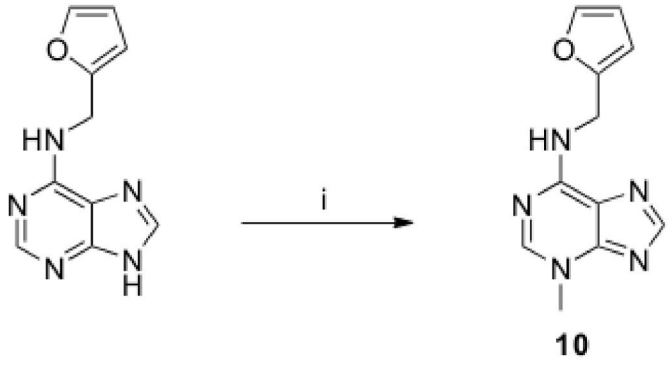


**Fig. 2.** Reagents and conditions: i) MeI, DMA, 85 °C, 2 days, 58 %.

for 14 h provided 6-furfurylamino-9-(tetrahydropyran-2-yl)purine (**VI**) which was further halogenated at purine C8 atom. A halogen atom was introduced using one-pot two step reaction by lithiation (LDA, THF, −78 °C, 1 h) followed by reaction with halogen donor (**15** – benzenesulfonyl chloride, **16** – $CBr_4$, **17** – $I_2$) in THF at −78 °C for 1 h. Reaction of **15** or **16** with aliphatic amines or alcoholates yielded 8-substituted 9-THP kinetins **18-31.** Introduction of phenylamino group (27) was achieved by application of Buchwald-Hartwig amination. Corresponding 8-substituted kinetins **32-44** were obtained after acid-catalysed hydrolysis of THP group (Fig. 4). Heating of 8-bromokinetin (**VII**) with sodium acetate in acetic acid at 120 °C for 1.5 day resulted in hydrolysis of bromine atom providing 8-oxokinetin **45**. Contrary to nucleophiles used in preparations of **18-31** (Fig. 4 v – xviii), nucleophilic attack on the C8 chlorine atom with ammonia in 8-chloro-9-THP-kinetin (**15**) is not possible. Direct ammonolysis of C8 chlorine atom of **IX** [6] and **X** [84] was achieved by stirring the starting compounds at room temperature for 1 day in *i*PrOH saturated at 0 °C by ammonia. The low reaction yield of **XII** (only 18 %) was caused by formation of 6-amino-2,8-dichloro-9-(tetrahydropyran-2-yl)purine as a by-product in 1:1 ratio and problems with their separation. Hereafter, substitution at *C*6 atom and hydrolysis of THP group resulted in formation of **47**, **49** (62 %, 83 %) and **48**, **50** (71 %, 83 %), respectively. 2, 8-Dichlorokinetin **46** was prepared from 2,6,8-trichloropurine (**VIII**) according to previously published protocol [34].

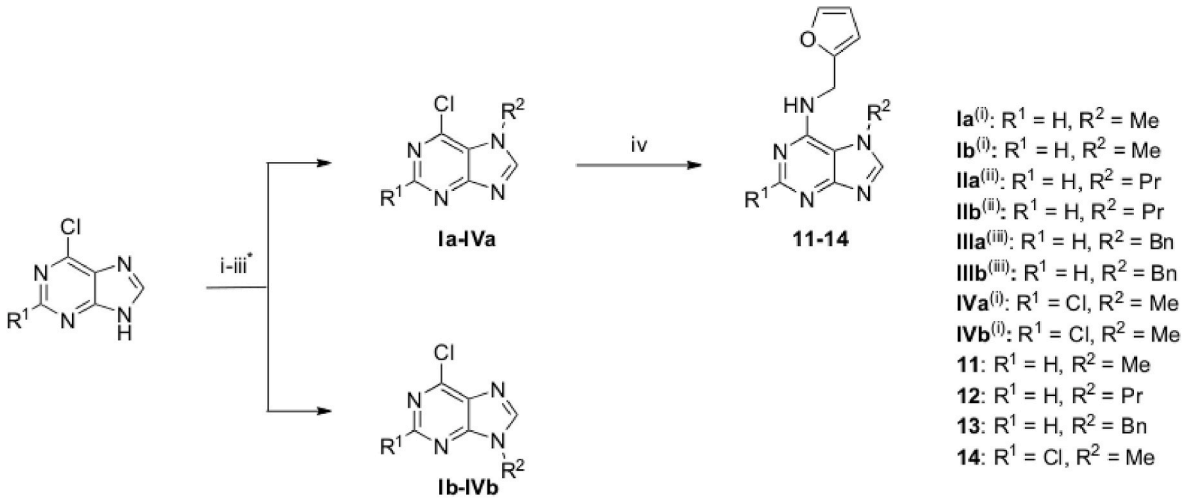


**Fig. 3.** Reagents and conditions: i) MeI, $K_2CO_3$, DMF, rt, overnight, 20 % (for Ia), 63 % (for Ib), 16 % (for IVa), 58 % (for IVb); ii) propyl iodide, $K_2CO_3$, DMF, rt, overnight, 16 % (for IIa), 55 % (for IIb); iii) benzyl chloride, $K_2CO_3$, DMF, rt, overnight, 18 % (for IIIa), 63 % (for IIIb); iv) furfurylamine, $Et_3N$, nPrOH, reflux, 4 h, 50 % (for 11), 54 % (for 12), 76 % (for 13), 43 % (for 14), * – various conditions.

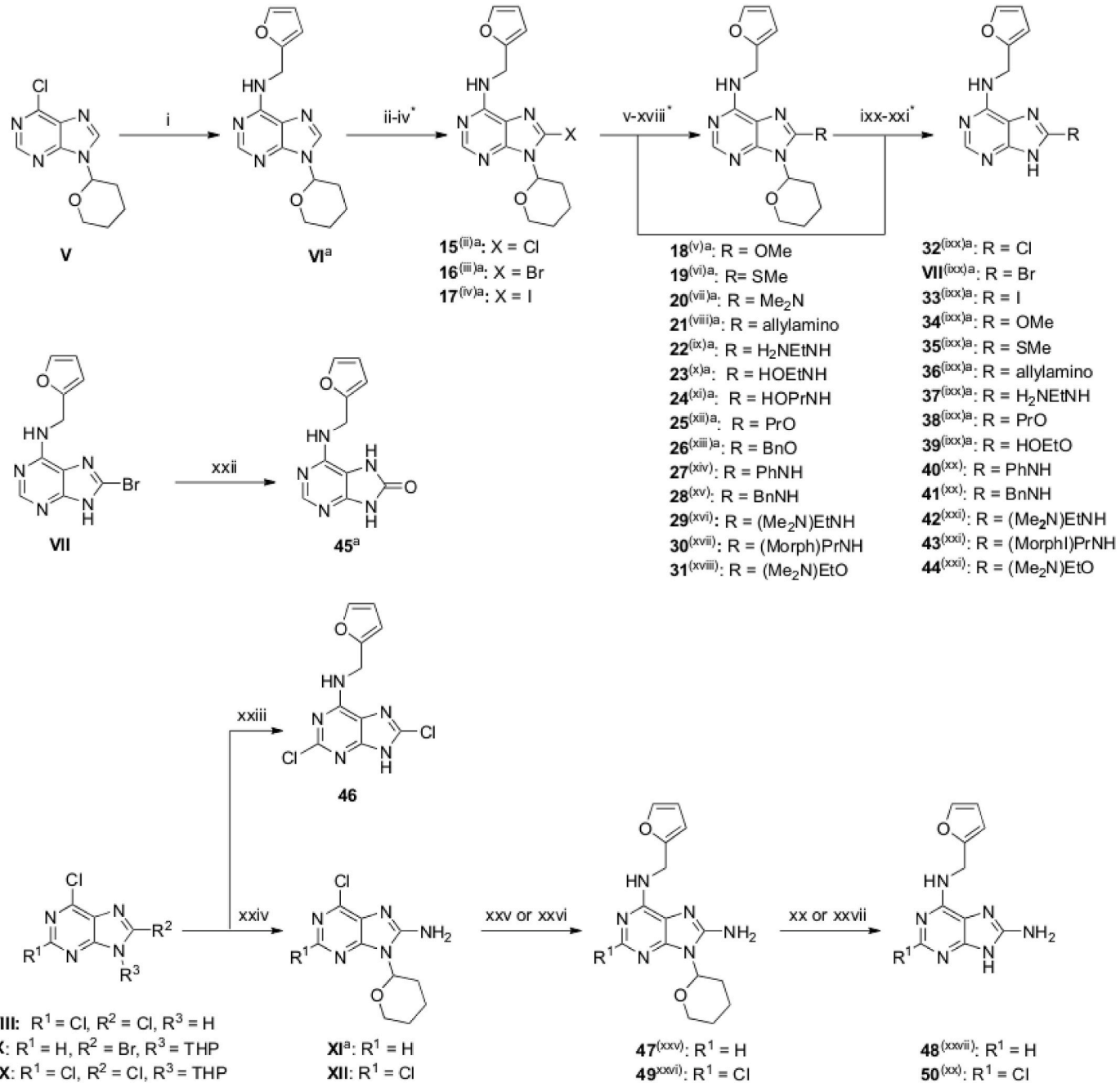


**Fig. 4.** Reagent and conditions: i) furfurylamine, $Et_3N$, nPrOH, 65 °C, 14 h; ii) LDA, THF, −78 °C, 1 h/benzenesulfonyl chloride, −78 °C, 1 h, 69 %; iii) LDA, THF, −78 °C, 1 h/$CBr_4$, -78 °C, 1 h, 37 %; iv) LDA, THF, −78 °C, 1 h/$I_2$, -78 °C, 1 h, 66 %; v) KOtBu, MeOH, 60 °C, 10 h, 73 %; vi) NaSMe, iPrOH, 45 °C, 2.5 h, 96 %; vii) $Me_2NH$, MeOH, rt, overnight, 83 %; viii) allylamine, 60 °C, 10 h, 58 %; ix) ethane-1,2-diamine, 50 °C, 35 min, 77 %; x) 2-aminoethanol, 80 °C, 75 min, 56 %; xi) 3-aminopropanol, 60 °C, 6 h, 90 %; xii) NaOH, nPrOH, 60 °C, overnight, 65 %; xiii) BnOH, Na, 65 °C, overnight, 20 %; xiv) aniline, Xantphos, $Pd_2(dba)_3$, NaOtBu, 2-MeTHF, 77 °C, 3.5 h, 20 %; xv) $BnNH_2$, $Et_3N$, iPrOH, 80 °C, 2.5 days, 69 %; xvi) 2-(dimethylamino)ethylamine, $Et_3N$, iPrOH, 80 °C, 1.5 days, 79 %; xvii) 3-morpholinopropylamine, $Et_3N$, iPrOH, 80 °C, 30 h, 89 %; xviii) 2-(dimethylamino)ethanol, NaH, toluene, rt, 3 days, 60 %; ixx) AcOH, water, rt, overnight, 19 % (for 32), 66 % (for VII), 97 % (for 33), 60 % (for 34), 78 % (for 35), 42 % (for 36), 88 % (for 37), 31 % (for 38), 31 % (for 39); xx) 10 % HCl, MeOH, rt, 2 days, 37 % (for 40), 58 % (for 41), 71 % (for 48); xxi) 10 % HCl, MeOH, water, 60 °C, 2 h-1 day, 76 % (for 42), 90 % (for 43), 91 % (for 44); xxii) AcOH, NaOAc, 120 °C, 1.5 days, 16 %; xxiii) furfurylamine, water, reflux, 0.75 h; xxiv) isopropanolic ammonia, rt, 1 day, 50 % (for XI), 18 % (for XII); xxv) furfurylamine, DIPEA, tBuOH, 100 °C, 7 days, 62 %; xxvi) furfurylamine, 45 °C, 1.5 h, 83 %; xxvii) HCl, MeOH, 50 °C, 20 h, 71 %, * – various conditions, [a] [17].

As mentioned above, reaction of 6-chloropurine or 2,6 dichloropurine with haloalkanes in the presence of $K_2CO_3$ in DMF afforded N7 derivatives (**Ia-IVa**) as a minor product and N9 isomers (**Ib-IVb**) as the main products (yield 55–63 %) (Fig. 3), **Ib-IIIb** were further converted into corresponding kinetin derivatives **51-53** using focused microwave irradiation in reasonable yields (57–79 %) (Fig. 5). Syntheses of other N9 derivatives **54**, **55, 58–61** [18] and **56** [19] were described in our previous publications. Compound **57** was prepared simply by the reaction of **1** with 1-bromo-3-chloropropane in $K_2CO_3$/DMSO conditions, whereas 9-aminoalkyl kinetins **62, 63** were prepared in three steps using a modified protocol [7]. Firstly, 6-chlorpurine was alkylated by *N*-Boc protected aminoalcohols under Mitsunobu conditions ($PPh_3$, DIAD, THF) providing **XV** and **XVI** in a good yield followed by substitution at *C*6 atom giving **XVII** and **XVIII** in very good to excellent yield.

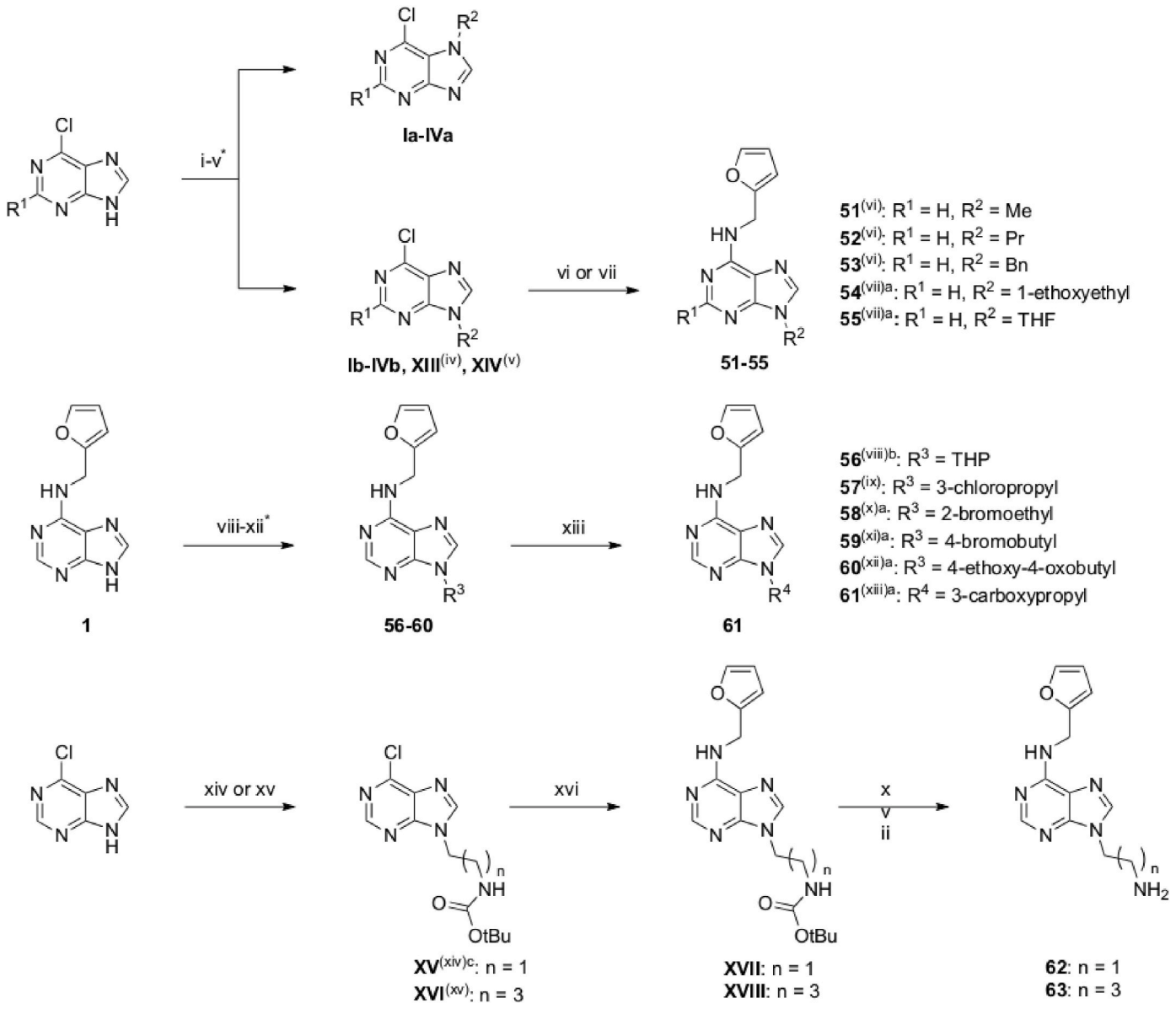


**Fig. 5.** Reagents and conditions: i) MeI, $K_2CO_3$, DMF, rt, overnight, 20 % (for Ia), 63 % (for Ib), 16 % (for IVa), 58 % (for IVb); ii) propyl iodide, $K_2CO_3$, DMF, rt, overnight, 16 % (for IIa), 55 % (for IIb); iii) benzyl chloride, $K_2CO_3$, DMF, rt, overnight, 18 % (for IIIa), 63 % (for IIIb); iv) ethyl vinyl ether, pTsOH, EtOAc, 55 °C, 2 h, 65 %; v) 2,3-dihydrofuran, TFA, EtOAc, rt, 1 h, quantitative; vi) furfurylamine, $Et_3N$, MeOH, MW, 120 °C, 15 min, 79 % (for 51), 57 % (for 52), 67 % (for 53); vii) furfurylamine, $Et_3N$, nPrOH, reflux, 3 h, 70 %; viii) 3,4-dihydro-2H-pyran, HCOOH, EtOAc, reflux, 3 h, 76 %; ix) 1-bromo-3-chloropropane, $K_2CO_3$, DMSO, rt, overnight, 60 %; x) 1,2-dibromoethane, $K_2CO_3$, DMF, rt, overnight; xi) 1,4-dibromobutane, $Cs_2CO_3$, DMSO, rt, overnight; xii) ethyl 4-bromoacetate, $Cs_2CO_3$, DMF, rt, overnight; xiii) NaOH, 50 % EtOH, rt, overnight; xiv) 2-(Boc-amino)ethanol, $Ph_3P$, DIAD, THF, rt, 2 h, 68 %; xv) 4-(Boc-amino)butanol, $Ph_3P$, DIAD, THF, rt, 2 h, 67 %; xvi) furfurylamine, $Et_3N$, nPrOH, reflux, 4 h, 90 % (for XVII), 81 % (for XVIII); q) Dowex 50W X8, DCM, reflux, 5 h/4 M methanolic ammonia, rt, overnight, 78 % (for 62), 51 % (for 63); * – various conditions, [a] [18], [b] [19], [c] [7].

Simultaneous deprotection and purification of Boc-amines was achieved on strong cation exchange resin Dowex 50W X8 [64].

Compounds **65-68** and **69-72** [10] were prepared by substitution of chlorine atom at *C*6 atom of 6-chloropurine, 6-chloropurine riboside and/or 6-chloro-9-(tetrahydrofuran-2-yl)purine with corresponding amines and $Et_3N$ in *n*PrOH under elevated temperature (Fig. 6). Finally, **73** was obtained by heating of 9-(tetrahydrofuran-2-yl)adenine (**IXX**) with furan-2-carbonyl chloride at 130 °C for 7 h in a 77 % yield, similarly to the described procedure [95].

### 2.2. Effects of the compounds on the splicing of mutant ELP1 transcript

The effects of kinetin derivatives on ELP1 exon 20 inclusion were evaluated in the patient-derived fibroblast cell line GM04663. Reverse transcription and PCR (RT-PCR) with primers flanking exon 20 of ELP1 cDNA was followed by comparison of the amounts of the PCR products corresponding to the wild-type transcript and aberrant transcript missing exon 20 [81]. During the screening and structure-activity exploration phase of the study, the activity of the compounds at 50 $\mu$M was evaluated semi-quantitatively using agarose gel electrophoresis (data not shown). This data was used for planning of synthesis of novel derivatives. In the end, the effect of the identified active compounds was validated and quantified using capillary electrophoresis; the concentration of the test compounds was 10 $\mu$M (Fig. 7). The performance of the assays was validated using positive controls kinetin (**1**) and 2-chlorokinetin (RECTAS, **2**).

The following structure-activity relationships emerged. Active compounds can be obtained by the substitution at the C2 atom of the purine

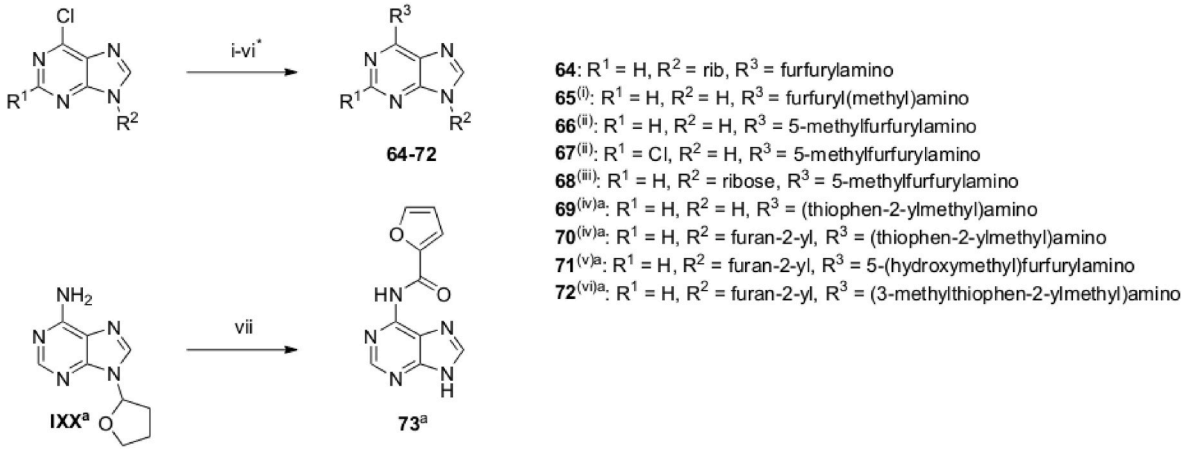


**Fig. 6.** Reagents and conditions: i) furfuryl(methyl)amine, $Et_3N$, nPrOH, reflux 5 h, 40 %; ii) 5-methylfurfurylamine, $Et_3N$, nPrOH, 100 °C, 4 h, 95 % (for 66), 97 % (for 67), 72 % (for 68); iii) 5-methylfurfurylamine, $Et_3N$, nPrOH, 85 °C, 5 h, 72 %; iv) 2-thiophenemethylamine, $Et_3N$, nPrOH, reflux, 4 h or 5 h, 65 % (for 69), 61 % (for 70); v) 5-(hydroxymethyl)furfurylamine, $Et_3N$, nPrOH, reflux, 5 h, 65 %; vi) 3-methylthiophene-2-methylamine, $Et_3N$, nPrOH, reflux, 6 h, 46 %; vii) furan-2-carbonyl chloride, pyridine, 130 °C, 7 h, 77 %, * – various conditions, [a] [10].

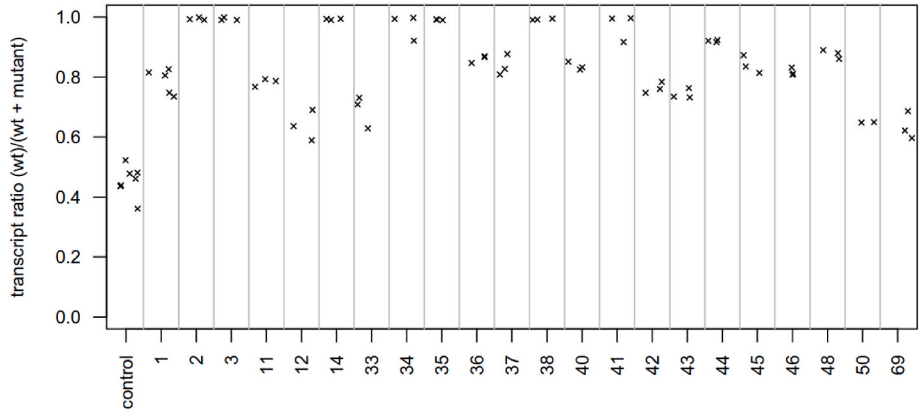


**Fig. 7.** The effect of kinetin and its derivatives (10 μM) that were identified in the screening phase as active on the ratio of the wild-type and mutant ELP1 transcripts as evaluated by capillary electrophoresis. Treatment with each compound led to increase in exon 20 inclusion, which was always statistically significant (adjusted p-values <0.05) with exception of the compounds 12, 33, 50 and 69.

of kinetin (**1**) by chlorine (**2**) or fluorine (**3**). On the other hand, derivatives with methylthio (**4**), amino (**5**), methylamino (**6**), dimethylamino (**7**) and substituted alkylamino (**8**, **9**) groups at this position were inactive. Substitution by methyl group at the atoms N3 (**10**) or N9 (**51**) caused a loss of the activity. The compounds **52–64** with larger substituents (alkyls, substituted alkyls and ribosyl) at the atom N9 were also inactive. On the other hand, the atom N7 allowed substitution by the methyl group (derivatives **11**). 7-Propyl derivative **12** was less active and N7-benzyl derivative **13** lost the activity completely. The combination of 2-chloro and 7-methyl group provided a derivative significantly more active than kinetin (**14**).

Active derivatives were also obtained by substitution at the C8 atom (**33–45**) with diverse groups, including halogens, amino, hydroxy, alkoxy and alkylamino groups. Among them, the benzylamino (**41**), methylthio (**35**), methoxy (**34**), and propoxy (**38**) derivatives were significantly more active than kinetin. However, the combination of C8-substitution with 9-tetrahydropyran-2-yl moiety led to inactive compounds (**15–31**). On the other hand a substitution at the atom C8 can be combined fruitfully with 2-chloro substitution as demonstrated by 2,8-dichloro (**46**) and 2-chloro-8-aminokinetin (**50**). A large group of other active 2,8-disubstituted derivatives was revealed in recently granted patent by Slaugenhaupt *et al.* [4], which also includes compounds **2** (RECTAS), **3** and **4**.

The observed permissivity of the position 8 to substitution including large groups (e.g. **43** morpholin-4-ylpropylamino group) suggests that this part of molecule is oriented in the active site of the unknown molecular target toward the cytosol. This observation inspired an idea to test derivatives where the imidazole of purine moiety is absent (**74–82**, Fig. 8, Supplementary Fig. S1). Indeed, several 4-chloropyrimidine derivatives were active at 50 $\mu$M (Fig. 9). However, substitution at the position 4 of the pyrimidine moiety with methyl or phenyl groups yielded inactive compounds. To our disappointment, diuretic drug furosemide, a derivative of 4-chloro-2-furfurylaminobenzoic acid was inactive. Other inactive compounds included all three positional isomers of furfurylaminopyrimidine. Methylation of the $N^6$ nitrogen of kinetin yielded compound **65** with no activity and the derivative with furan-2-carboxamido group at *C*6 was inactive as well (**73**). Also a substitution of the furan ring with 5-methyl (**66**, **67**) or 5-hydroxymethyl (**71**) group led to a loss of activity. Replacement of the furan ring with thiophene yielded derivative **69** with decreased activity.

Finally, plant hormones of other classes (auxin - 2-(indol-3-yl)acetic acid, gibberellin - GA9 and its methyl ester, brassinosteroid - brassinolide, and jasmonates - jasmonic acid and methyl jasmonate) were also tested. None of them corrected the aberrant ELP1 mRNA splicing (data not shown).

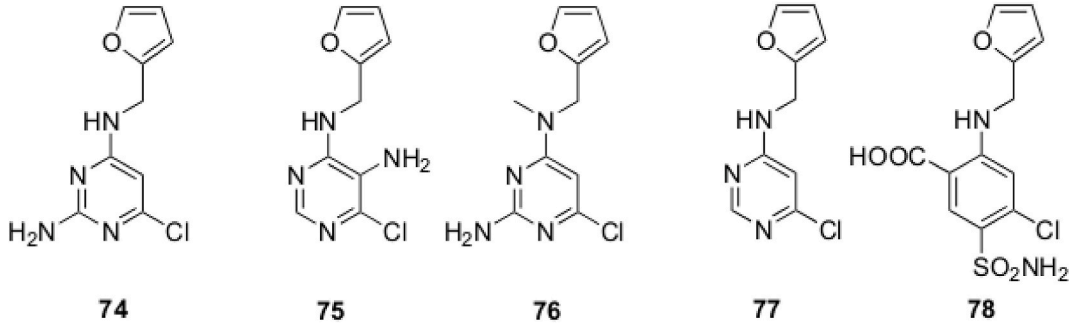


**Fig. 8.** The structures of the pyrimidine analogues of kinetin that induced increase in ELP1 exon 20 inclusion (**74–77**) and furosemide (**78**).

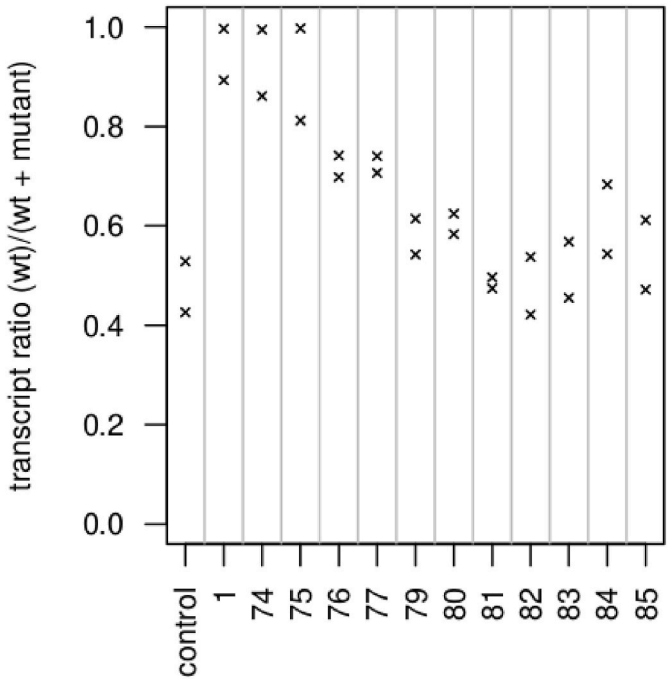


**Fig. 9.** The effect of the pyridine and pyrimidine analogues of kinetin (50 $\mu$M) on the ratio of the wild-type and mutant ELP1 transcripts evaluated by capillary electrophoresis. Kinetin (**1**) at 50 $\mu$M was used as a control. The effect was statistically significant (adjusted p-values <0.05) in the case of compounds of **1** and **74–77**.

### 2.3. Effect of the compounds on cell proliferation of non-malignant cells

A resazurin assay after 2-day incubation was used to evaluate the effect of the active compounds (50 $\mu$M) on proliferation of the GM04663 fibroblasts as well as several other non-malignant cell lines (skin fibroblasts BJ, keratinocytes HaCaT, and retinal epithelial cells ARPE-19). The assay is based on the fluorimetric quantification of resazurin reduction by mitochondria. The majority of the kinetin derivatives had no or limited (90–110 % of the signal of the control samples) effect on GM04663 fibroblasts. Only four compounds decreased resazurin signal by more than 20 % in any of the four cell lines (Supplementary Fig. S2). Those included 2-halogenated derivatives **2** and **3** and the derivatives with an aromatic substituent at C8 atom of the purine moiety (**40** - 8-phenylamino, **41**- 8-benzylamino).

### 2.4. In silico and in vitro pharmacokinetic modelling/prediction

For the majority (N = 22) of the active compounds, we performed biochemical assays used for a prediction of the ADME (absorption, distribution, metabolism and excretion) properties of (candidate) drugs sometimes collectively called pharmacokinetics *in vitro* assays [43,94]. The Parallel Artificial Membrane Permeability Assay (PAMPA) [92] is used for estimation of absorption by passive diffusion. The Caco-2 and MDCK-MDR1 permeability assays are established models of intestinal [24] and blood-brain barriers (BBB) [53], respectively. If both apical-to-basal and basal-to-apical permeabilities through the monolayers are studied, the assays can be used for identification of drugs removed from the cells by active efflux. Effective drug efflux is one of the characteristics of BBB. The prominent role plays MDR1 (P-gp, ABC1). To better simulate properties of BBB, dog kidney MDCK cells were transfected with human MDR1 [88]. The transporter make-up of differentiated colon carcinoma Caco-2 cells resembles that of enterocytes [76]. Metabolization by human plasma and liver microsomal fraction was used to evaluate the stability of the compounds. Finally, we also studied binding of the compounds to human plasma proteins. The results off all the assays are summarized in Supplementary Fig. S3.

Most of the compounds were highly stable in human plasma (<5 % degradation after 2 h). Degradation exceeded 10 % only in 4 cases (compounds **3**, **12**, **36**, **39**). Stability in the presence of the human liver microsomal fraction was variable (~67–100 % compound remaining after 1 h). Values for kinetin (**1**) and RECTAS (**2**) were comparable (89.9 and 96.1 %).

Marked differences (~19–96 %, mean = 56.9 %, sd = 24.2, median 18.9 %) were observed in plasma protein binding of the compounds. Fraction bound for kinetin (**1**) and more lipophilic RECTAS (**2**) were 55.6 % and 90.4 %, respectively. However, overall there was no clear relation between either stability or plasma protein binding and the values of the basic descriptors related to hydrophobicity and polarity including logP, molar refractivity and topological polar surface area (data not shown).

Permeability studies using PAMPA assay suggest moderate (- log $P_{app}$ 5–6 cm/s) or low ability (- log $P_{app}$ > 6 cm/s) to cross biological membranes by passive diffusion for **10** and **11** compounds, respectively. An exception is the derivative **42** with -log $P_{app}$ > 8 cm/s. Its tertiary amino group in the side chain at position 8 may be charged under the assay condition. Results of Caco-2 and MDR1-MDCK permeability assays offer a markedly different picture (Fig. 10).

With and exception of 2 derivatives, the compounds are expected to be absorbed from the gut (Caco-2 $P_{app}$ > 5 cm/s), 8 of them with high efficiency (Caco-2 $P_{app}$ > 20 cm/s). 16 compounds out the 22 are expected to cross blood-brain barriers (MDR1-MDCK Papp >10 cm/s). The high permeability of the cell barriers, in contrast to the artificial membrane, suggests that the compounds enter the cells through a transporter (s). It is tempting to speculate about active transport in the case of the compounds with extreme values in both cellular assays. Those include kinetin (**1**) but not RECTAS (**2**). *In silico* predictions provide further indirect support for existence of a transporter. BOILED-Egg approach [42] is based on the comparison of lipophilicity (expressed as logP) and polarity (expressed as tPSA) of test compounds with parameter boundaries derived from an analysis of brain and intestinal permeation of a large set

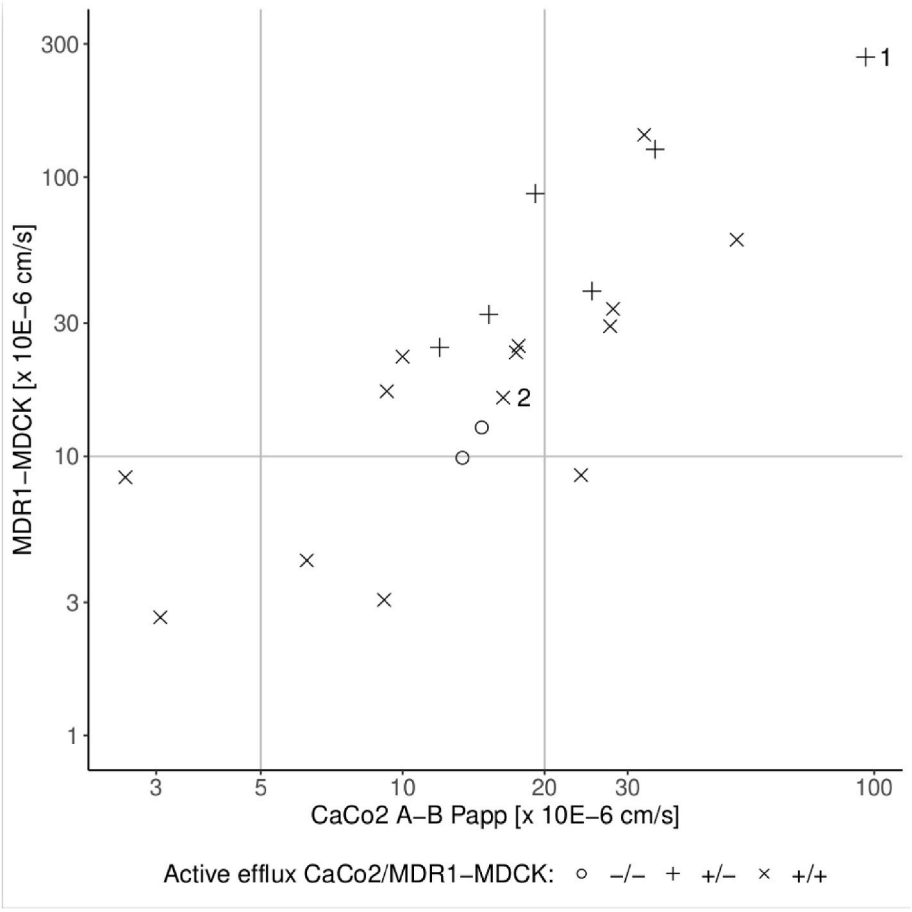


**Fig. 10.** A comparison of the results of the Caco-2 and MDR1-MDCK permeability assays for the active kinetin derivatives. The points corresponding to kinetin and RECTAS are labelled **1** and 2, respectively. The symbols indicate if a compound is a subject of the active efflux in none, either or both cell lines. The compounds with MDR1-MDCK permeability above 10 [uPapp] are predicted to cross the blood-brain-barrier. Vertical gray lines separate the compounds with predicted low, medium and high intestinal absorption.

of drugs. The model predicts brain permeation by passive diffusion only for two compounds (**12**, **46**) out of twenty two (Supplementary Fig. S4). We also observed that kinetin crosses MDR1-MDCK monolayer much better than its diverse purine isosteres [5]. Identification of the putative transporter(s) will be subject of follow-up studies. Here, we only note that cytokinin derived cyclin-dependent kinase inhibitors were shown to interact with nucleoside transporters [52] that beside nucleosides also transport nucleobases and various analogues of those.

Drug efflux probably further contributes to the overall low correlation between the PAMPA and the cellular permeability assays (Supplementary Fig. S5). Majority of the compounds are actively exported from the cells in both barrier models as indicated by efflux ratios >2 (Fig. 10). MDR1 efflux pump present in both cell lines maybe at least partially responsible [42]. Moreover cytokinin derived cyclin-dependent kinase inhibitors are known substrates of this transporter [8]. Different affinities for efflux transporter(s) could be another factor behind the marked differences in absorption of kinetin (**1**) and RECTAS (**2**).

### 2.5. RNA-seq study of the effects of 8-aminokinetin (compound 48)

We conducted an RNA-seq analysis with de novo assembly of the reads to investigate the effects of a 24 h treatment of GM04663 fibroblasts with compound **48** at 100 **μ**M concentration. Equimolar kinetin was included for comparison. The analysis focused on transcripts with a at least two-fold change expression at an adjusted p-value <0.05. The full list of differentially expressed transcripts, along with detailed results of Gene Ontology (GO) overrepresentation analysis performed at the gene level, is provided in the supplementary material (Tables S1–4, Figs. S6–11). Both compound **48** and kinetin increased the amount of wild-type ELP1 transcript. While kinetin treatment altered the expression of only 31 transcripts (24 upregulated, 7 downregulated), which did not belong to any coherent GO category clusters, the response to compound **48** was much more pronounced. This treatment significantly changed the expression of 324 transcripts (142 upregulated, 182 downregulated). Overrepresented GO categories (adjusted p-value <0.05) include “spliceosome complex” with majority of genes upregulated and 4 categories related to translation (Fig. 11A, Figs. S8–S10). Analysis of over-represented biological themes for upregulated genes reveals several other overlapping GO categories related to splicing and mRNA metabolism (Fig. 11B). The responsive mRNA splicing-related transcripts also included upregulated LUC7L and downregulated WDR70, which have been reported as sensitive to kinetin treatment by Boone *et al.* [99]. Other overrepresented categories are related to chromatin remodeling and phosphatidylinositol binding (Fig. S7).

## 3. Discussion

Familial dysautonomia is debilitating hereditary neurodegeneration with no causative therapy [9]. Slaugenhaupt *et al.* [81], reported that the molecular cause of the disease, the skipping of the exon 20 in the mutant ELP1 transcript, can be corrected by the treatment with phytohormones kinetin and $N^6$-benzyladenine. A positive effect of kinetin on the mutated target gene mRNA splicing was confirmed in animal model.

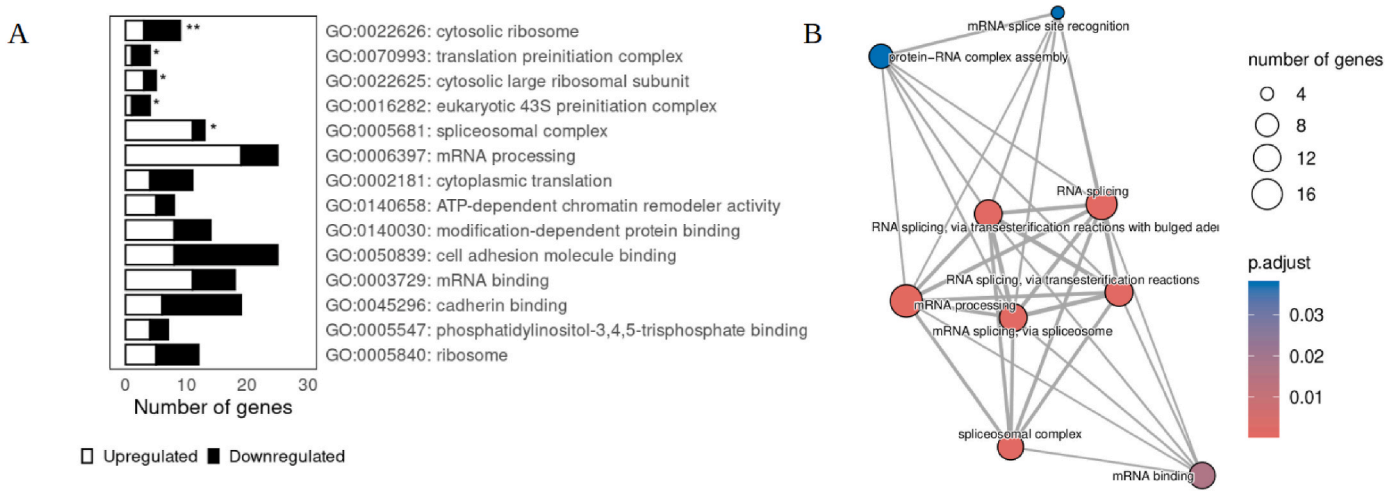


**Fig. 11.** Over-representation analysis of Gene Ontology categories for differentially expressed genes after treatment with compound **48.** A) Analysis of all differentially expressed genes. Adjusted p-value: ** - < 0.01, * <0.05. B) Relation between the mRNA splicing-related categories for upregulated genes.

The first published data from human studies show that treatment with kinetin increases levels of wild-type transcript in the patients' lymphocytes [29].

Yoshida *et al.* [91] later discovered a more potent kinetin derivative (2, 2-chlorokinetin, RECTAS), and two more active 6-substituted purines were reported by Salani *et al.* [75]. Another set of active $N^6$-substituted adenines and their analogues mainly with 2-chloro substitution was revealed in a recently granted patent by Slaugenhaupt *et al.* [4]. Purine isosteres of kinetin were explored by Maková *et al.* [5]. However, no systematic structure-activity study of kinetin derivatives has been published yet. Here we report synthesis and testing of a broad set of Lipinski rule-compliant kinetin substitution derivatives for their ability to correct aberrant splicing of the mutant ELP1 gene.

We found that active compounds can be obtained by substitution of position 2 of the purine ring not only by chlorine as in RECTAS but also with fluorine. Whereas a substitution of the positions 3 or 9 led to a loss of the activity, position 7 could be substituted by a small alkyl. Notably, the position 8 can be substituted by groups of diverse physico-chemical properties including large 8-alkylamino and 8-alkoxy substituents. This observation suggests that the position 8 is oriented out of the active site of the yet unknown molecular target. Therefore, we also tested several derivatives where the 5-membered ring is missing altogether and found that they retain some activity. They may serve as leads for new series with limited side-effects resulting from interaction(s) with the human purinome. The results in purine series also demonstrate that substitutions in the positions 7 or 8 can be successfully combined with 2-chloro substitution. The combination of 2-chloro substituent with a side chain in position 8 is also present in the two active compounds reported by Salani *et al.* However, in these compounds furan ring is replaced by another heterocycle.

The initial insights into ADME properties (absorption, distribution, metabolism and excretion) of the active compounds were obtained using the panel of *in vitro* assays. All the compounds were stable in human plasma. However, their stability in the presence of human liver microsomal fraction as well as plasma protein binding was highly variable with no clear structure-activity relationships.

Most of the compounds are predicted to cross biological barriers, including blood-brain barrier, according to the Caco-2 and MDCK-MDR1 models. Exceptionally high permeability of some compounds, including the parent kinetin, suggests that they enter the cells by facilitated diffusion or possibly active transport. The predicted high bioavailability of kinetin seems to be in concord with experimental data – kinetin is efficiently absorbed after peroral administration and animal studies confirmed its ability to cross BBB [3]. On the other hand, absorption of some of the compounds may be limited by active efflux – those include compound **2**, RECTAS. Notably, the substitution of RECTAS by the 8-amino group reverses this effect. Follow-up mechanistic studies will undoubtedly shed more light on the transport mechanisms of kinetin and its derivatives. The putative import mechanism may be both opportunity and obstacle in optimization of kinetin derivatives for treatment of neurodegenerations including familial dysautonomia, parkinsonism [47] and Huntington disease [33].

Previous studies have shown that kinetin has only a limited effect on gene expression. Boone *et al.* [99] used Whole Human Genome Microarray Kit, 4 × 44K (Agilent) to study the effect of 48 h treatment of 100 $\mu$M kinetin in patient olfactoryecto-mesenchymal stem cells. Expression of only 12 genes was changed by factor two or more. Seventy-two genes had absolute value of fold change over 1.5. Besides ELP-1 they included also several genes related to splicing: LUC7L, SNRPA and WDR70 with respective fold change of 2.04, −1.70 and −1.52. A recent study demonstrated that the effects of RECTAS (**2**) on mRNA pool is also limited and splicing modulation is very specific [2].

We conducted an RNA-seq analysis of a 24 h treatment of patient fibroblasts with compound **48** (8-aminokinetin) at 100 $\mu$M with kinetin as a comparator. In contrast to kinetin, compound **48** induced much more profound changes in gene expression (31 vs. 324). Notably the over-represented Gene Ontology categories are related to cell components and biological processes related to alternative mRNA splicing, with the majority of genes upregulated. Other influenced processes are related cytosolic translation and chromatin remodeling. Although treatment with compound **48** did not have a significant negative effect on fibroblast viability during a 2-day toxicity test (section 2.3), our unpublished long-term cultivation studies show that the compound **5** in contrast to kinetin has a negative effect on cell proliferation. Thus we cannot exclude the possibility of toxic effects related to translation and/or chromatin perturbation especially with long-term use of the drug for familial dysautonomia. Overall, these results suggest that compound **48** may influence mRNA splicing also through a mechanism distinct from that of kinetin which may possibly contribute to the therapeutic effect. However, a less specific effect on mRNA splicing may also be a source of side effects.

## 4. Experimental

### 4.1. Chemistry

Synthetic procedures and NMR spectra for the newly prepared compounds are summarized in the Supplementary Information. Purine

intermediates were prepared according to the previously published protocols: **V** [85], **VIII**, **IX** [6], **X** [84], **XV** [7], **IXX** [10]. The following substances were provided by L. Zahajská **15-26**, **32-39, 45**, V. Mik **54, 55, 58–61** [18], L. Plíhalová **56** [19] and M. Hönig **69-72** [10]. Finally **1** and **64** were purchased from OlChemIm Ltd and **74-85** from Molport.

### 4.2. Cell culture

GM04663, a skin fibroblast cell line homozygous for the 2507+6T > C mutation in ELP1 gene derived from a 2-year old female with familial dysautonomia, was obtained from Coriell repository. Skin fibroblast BJ (ATCC® CRL-2522™), retinal pigment epithelium cells ARPE-19 (ATCC® CRL-2302) and epithelial colorectal adenocarcinoma cells Caco-2 (ATCC® HTB-37™) were from American Type Culture Collection. Keratinocytes HaCaT were from DKFZ Cell Line Service. MDR1 transfected canine kidney cells MCDK were from Netherlands Cancer Institute.

The cells were maintained in Dulbecco's modified Eagle' medium (DMEM) or in DMEM/F12 medium in the case ARPE-19, containing 5 g/L glucose, 2 mM L-glutamine, 100 U/mL penicillin, 100 μg/mL streptomycin and 10 % fetal calf serum (Sigma) in standard culture conditions (5.5 % $CO_2$, 37 °C, 100 % relative humidity). The cells were subcultured twice a week.

### 4.3. Evaluation of cytotoxicity of the compounds

Toxicity of the compounds to GM04663, BJ, HaCaT, ARPE-19 cells was evaluated using a standard assay based on the metabolic reduction of non-fluorescent resazurin into highly fluorescent resofurin [31]. The cells were trypsinized and dispensed into 96-well plates (5000 cells in 80 **μ**L of medium per well). After 24 h, 5 × concentrated solution of the test compounds in the culture medium were added (the final concentration 50 μM). DMSO vehicle served as a negative control. After 48 h, 20 μL of 11 × concentrated solution of resazurin (Sigma) in the culture medium was added to the cells into the final concentration of 0.0125 mg/mL. Fluorescence (ex = 570 nm, em = 610 nm) was measured after 1h (ARPE-19) or 3 h (HaCaT and BJ) incubation using M2 reader (Biotek).

### 4.4. Evaluation of the effect of the compounds on ELP1 transcript alternative splicing

About 500.000 GM04663 cells were seeded in 10 cm Petri dishes and grown overnight before the treatment with the test compounds. Kinetin (**1**) and 2-chlorokinetin (**2**, RECTAS) were used as positive controls. DMSO vehicle served as a negative control. After 24 h, total RNA was extracted from the cells using Trizol reagent. Isolated RNA was transcribed to cDNA using High Capacity cDNA Reverse Transcription Kit (Applied Biosystems). Polymerase chain reaction with primers 5′-CAGGTGTCGCTTTTTCATCA-3′ and 5′-CATTTCCAAGAAA-CACCTTAGGG-3′ [22] was used to amplify a ELP1 cDNA segment between nucleotides 2194 and 2593 (numbering corresponding to NM_003640.5. transcript). The conditions of the PCR reaction using JumpStart *Taq* DNA Polymerase with $MgCl_2$ (Sigma-Aldrich) were as follows: initial denaturation at 94 °C for 5 min followed by 34 cycles (denaturation at 94 °C for 40 s, annealing at 63.8 °C for 30 s and elongation at 72 °C for 90 s) with final incubation at 72 °C for 5 min. The PCR products corresponding to wild-type transcript (422 bp) and transcript without exon 20 (348 bp) were separated by agarose gel electrophoresis (1.5 % gel) and visualized by GelRed staining. For the final comparison of the compounds identified as active during the screening and structure-activity exploration phase, microfluidic electrophoresis (Agilent 2100 Bioanalyzer with 1000 LabChip kit) was used. A comparison with DNA standards of a known size and concentration allowed for the precise quantification of the wild-type and aberrant transcripts concentrations.

### 4.5. In vitro ADME assays

#### 4.5.1. Analytical chemistry

Preparation of the lyophilized samples for the analysis is described in the sections dedicated to the individual *in vitro* ADME methods. Quantification of the test compounds in the samples was performed using RapidFire RF300 system (Agilent Technologies) interfaced with QTRAP 5500 mass spectrometer fitted with an electrospray ionization source (AB Sciex, Concord, Canada) and running in multiple – reaction monitoring mode.

Lyophilized samples were dissolved in the mobile phase (95 % water, 5 % acetonitrile, 0.1 % formic acid) with respective internal standards. The dissolved samples were aspired directly from 96-well plates into a 10 μL sample loop and passed through a C4 cartridge (Agilent Technologies) with solvent A (95 % water, 0.01 % formic acid, 5 % acetonitrile) at a flow rate of 1.5 mL/min for 3 s. After the desalting step, the analyte retained on the cartridge was eluted with solvent B (95 % acetonitrile, 5 % 0.01 % formic acid) to the mass spectrometer at a flow rate of 0.4 mL/min for 7 s. Mass spectrometry was carried out using electrospray ionization in the positive ion mode. Daughter ion peaks were identified using a multiple – reaction monitoring protocol.

#### 4.5.2. Chemical stability

Two μM solutions of the test compounds in PBS buffer (pH 7.4) were incubated for 0, 15, 30, 60 and 120 min at 37 °C. The reactions were stopped by the addition of cold methanol, and the samples were lyophilized.

#### 4.5.3. Stability in human plasma

Two μM solutions of the test compounds were incubated with human plasma (Transfusion Department, University Hospital, Olomouc, Czech Republic) for 0, 15, 30, 60 and 120 min at 37 °C. The reactions were stopped by addition of acetonitrile–methanol mixture (2:1). Samples were stored at -80 °C overnight and centrifuged (2811×*g*, 6 min, 4 °C). Supernatants were lyophilized.

#### 4.5.4. Microsomal stability

The reaction mixtures of test compounds (2 μM), human liver microsomes (ThermoFisher Scientific, 0.5 mg/mL), NADPH generating system ($NADP^+$ - 0.5 mM, isocitrate dehydrogenase - 6 U/mL, isocitric acid – 4 mM, and $MgSO_4$ – 5 mM) in 0.1 mol/L $K_3PO_4$ buffer. The reactions were stopped by the addition of acetonitrile–methanol mixture (2:1) after 0, 15, 30, and 60 min at 37 °C. The samples were centrifuged (2811×*g*, 6 min, 4 °C) and the supernatants were lyophilized.

Calculations: The intrinsic clearance was calculated as $CL_{int} = V^*(0.693/t_{1/2})$, where V is the volume of the reaction in μL related to the weight of the microsomal protein in mg per reaction. Elimination half-life was calculated using the equation $t_{1/2} = 0.693/k$, where k is the slope of linear regression of natural logarithm of percent substrate remaining plotted versus incubation time [90].

#### 4.5.5. Parallel artificial membrane permeability assay

The parallel artificial membrane permeability assay (PAMPA) was performed using the Millipore MultiScreen filter MultiScreen-IP Durapore 0.45 μm plates and receiver plates (Merck Millipore) according to the manufacturer's protocol PC040EN00. The test compounds were dissolved in PBS (pH 7.4) to the final concentration of 20 μM and added to the donor wells. The filter membrane was coated with 10 % lecithin (Sigma Aldrich) dissolved in dodecane and the acceptor wells were filled with PBS (pH 7.4). The acceptor filter plate was carefully placed on the donor plate. Following 18 h incubation at the room temperature aliquots of acceptor and donor solutions were removed and lyophilized.

Calculations: The relative permeability logPe was calculated as $\log Pe = \log\{C \times -\ln(1-drug_A/drug_E)\}$, where $C = (V_A \times V_D)/\{(V_D + V_A) \times A \times T\}$. $V_D$ and $V_A$ are the volumes of the donor and acceptor solutions, respectively, A is the active surface area in $cm^2$ and T is time of

the incubation in seconds. DrugA and drugE is the mass of the compound in the acceptor solution and in the solution in theoretical equilibrium (as if the donor and acceptor were combined), respectively.

#### 4.5.6. Protein plasma binding assay

The assay is based on the rapid equilibrium dialysis (RED) [59]. The RED plate inserts (Thermo Scientific™, Rockford, USA) consist of two chambers separated by a semipermeable membrane. For each compound, 10 $\mu$M in 10 % human plasma was transferred into the one chamber and the other was filled with PBS buffer (pH 7.4). The equal volumes of the solutions from either compartment were transferred into microtubes after the 4 h incubation with shaking (250 rpm). Either 10 % plasma or PBS buffer (pH 7.4) was added so that all the samples had the same matrix. The reactions were stopped by the addition of acetonitrile-methanol mixture (2:1). The samples were centrifuged (2811×*g*, 6 min, 4 °C) and the supernatants were lyophilized.

#### 4.5.7. Studies of the transport across Caco-2 and MDR-MDCK cell monolayers

In order to generate cell monolayers for transport studies [24,53], the cells were trypsinized and seeded on tissue culture polyester membrane filters (pore size 0.4 $\mu$m for Caco-2 and 1 $\mu$m for MDR1-MCDK) in 96-well Transwell® plates (Corning, NY, USA). The culture medium was added to both the donor and the acceptor compartments and the cells were allowed to differentiate and form the monolayers. The culture medium was changed every other day.

Caco-2 and MDR1-MCDK differentiated monolayers were used only if they were intact, which was confirmed by Lucifer Yellow Rejection Assay. Prior to the experiment, the cells were washed twice with Hank's balanced buffer solution (HBBS) (Gibco, Waltham, USA) and pre-equilibrated with HBSS buffer at pH 7.4 for 1 h. After removing the medium, the cells were treated with 10 $\mu$M test compounds in HBSS (pH 7.4) for 1 and 2 h, for MDCK and Caco-2, respectively. Thereafter, the samples were removed from both donor and acceptor compartments and lyophilized. All experiments were done in duplicate.

Calculations: The apparent permeability coefficient was calculated as $P_{app} = (dQ/dt)/(C_0 \times A)$, where dQ/dt is the rate of permeation of the drug across the cell monolayer, $C_0$ is the donor compartment concentration at time t = 0 and A is the area of the cell monolayer. The efflux ratio R was defined as ratio $P_{BA}/P_{AB}$ where $P_{BA}$ and/$P_{AB}$ represent the apparent permeability of test compound from the basal to apical and apical to basal side of cell monolayer, respectively. The compounds with the efflux ratio of 2 or higher were considered as potential P-gp substrates.

### 4.6. Data analysis

Molecular descriptors were calculated using rdkit, a Python package for cheminformatics (https://www.rdkit.org). Data handling, analysis and visualization was done in R (https://www.r-project.org) with the exception of the calculations of ADME parameters that were done in Microsoft Excel. A BOILED-egg implementation available at http://www.swissadme.ch [42] was used for prediction of BBB permeability and interaction with MDR1. The effects of the compounds on the increase in the ratio of the wild-type to total ELP1 transcript were evaluated by a strict non-parametric method with a correction for multiple testing described by Konietschke *et al.* [58] and implemented in nparcomp R library. One-sided test, Dunnett-type contrasts and Fisher-approximation were used. Differences with the corrected p-values $<0.05$ were considered statistically significant. Standard errors for drug efflux ratios were calculated by the Delta method described in [89] implemented in R.

### 4.7. Transcriptomics study

Approximately 500,000 GM04663 cells were seeded in 10 cm Petri dishes and grown overnight before treatment with 100 $\mu$M compound **48** and kinetin (**1**). DMSO served as a negative control. After 24 h, total RNA was extracted from the cells using Trizol reagent. The extracted total RNA was used for cDNA library preparation with the Illumina® TruSeq® Stranded mRNA Sample Preparation Kit (Illumina, San Diego, CA, USA). Library construction and sequencing of the samples were performed on the Illumina HiSeq 2000 platform in 100-base paired-end mode. Three replicates were sequenced for each condition, except for kinetin, where five samples were used. This decision was based on our previous unsuccessful attempt to identify genes sensitive to kinetin in BJ fibroblasts using Illumina Human v4 arrays. Fastq reads obtained from RNA-seq underwent quality trimming and adaptor removal using Cutadapt (version 2.1) with parameters set to maintain a minimum Phred quality score of 30 and a minimum read length of 50 nucleotides. Trimmed reads were aligned to the human reference genome (hg38) using STAR aligner (version 2.7.11b). Stringtie (version 2.2.0) was employed for splice isoform reconstruction based on the aligned reads. Gene expression levels were quantified using Salmon (version 1.10.2) on the transcript models reconstructed by Stringtie [11]. Sleuth (version 0.30.0) was utilized for normalization of read counts and subsequent differential gene expression (DGE) analysis [12–14,101,102]. For subsequent analysis, human transcripts were considered differentially expressed if the absolute estimated fold change (b-value) was greater than 2 and the adjusted p-value was less than 0.05. Overrepresentation analysis for pooled Gene Ontology categories was carried out using the ClusterProfiler Bioconductor package [15]. Packages org.Hs.eg.db [16] and GO.db [103] (Carlson, 2019b) were used for annotation. Heat maps were generated using the pheatmap package.

## CRediT authorship contribution statement

**Barbara Maková:** Writing – original draft. **Václav Mik:** Writing – original draft. **Barbora Lišková:** Investigation. **Lenka Drašarová:** Investigation. **Martina Medvedíková:** Investigation. **Alena Hořínková:** Investigation. **Petr Vojta:** Formal analysis. **Marek Zatloukal:** Investigation. **Lucie Plíhalová:** Investigation. **Martin Hönig:** Investigation. **Karel Doležal:** Investigation. **Kristýna Forejt:** Investigation. **Tomáš Oždian:** Investigation. **Marián Hajdúch:** Formal analysis. **Miroslav Strnad:** Formal analysis. **Jiří Voller:** Writing – original draft, Supervision.

## Declaration of competing interest

The authors declare that they have no known competing financial interests or personal relationships that could have appeared to influence the work reported in this paper.

## Acknowledgement

The research was supported by grants CZ-OPENSCREEN — LM2018130 by Czech Ministry of Education and Sport and project nr. LX22NPO5107 (MEYS): Financed by EU – Next Generation EU. And project IGA_2024_005 by Palacký University Olomouc.

We are grateful to Kateřina Faksová for excellent technical assistance.

## Appendix A. Supplementary data

Supplementary data to this article can be found online at https://doi.org/10.1016/j.ejmech.2024.117176.

## Data availability

Data will be made available on request.

## References


[1] A. Hamosh, J.S. Amberger, C. Bocchini, A.F. Scott, S.A. Rasmussen, Online mendelian inheritance in man (OMIM®): victor McKusick's magnum opus, Am. J. Med. Genet. 185 (11) (2021) 3259–3265, https://doi.org/10.1002/ajmg.a.62407.

[2] M. Ajiro, T. Awaya, Y.J. Kim, K. Iida, M. Denawa, N. Tanaka, R. Kurosawa, S. Matsushima, S. Shibata, T. Sakamoto, L. Studet, A.R. Krainer, M. Hagiwara, Therapeutic manipulation of IKBKAP mis-splicing with a small molecule to cure familial dysautonomia, Nat. Commun. 12 (1) (2021) 4507, https://doi.org/10.1038/s41467-021-24705-5.

[3] R.S. Shetty, C.S. Gallagher, Y.-T. Chen, M.M. Hims, J. Mull, M. Leyne, J. Pickel, D. Kwok, S.A. Slaugenhaupt, Specific correction of a splice defect in brain by nutritional supplementation, Hum. Mol. Genet. 20 (21) (2011) 4093–4101, https://doi.org/10.1093/hmg/ddr333.

[4] S.A. Slaugenhaupt, G. Johnson, W.D. Paquette, W. Zhang, J. Marugan, Compounds for Improving mRNA Splicing, US Patent US20230279007, 2020.

[5] B. Maková, V. Mik, B. Lišková, G. Gonzalez, D. Vítek, M. Medvedíková, B. Monfort, V. Ručilová, A. Kadlecová, P. Khirsariya, Z.G. Barreiro, L. Havlíček, M. Zatloukal, M. Soural, K. Paruch, B. DÁutréaux, M. Hajdúch, M. Strnad, J. Voller, Cytoprotective activities of kinetin purine isosteres, Bioorg. Med. Chem. 33 (2021) 115993, https://doi.org/10.1016/j.bmc.2021.115993.

[6] J.M.J. Nolsøe, L.L. Gundersen, F. Rise, Synthesis of 8-halopurines by reaction of lithiated purines with appropriate halogen donors, Synth. Commun. 28 (23) (1998) 4303–4315, https://doi.org/10.1080/00397919808004464.

[7] K. Kubiasová, V. Mik, J. Nisler, M. Hönig, A. Husičková, L. Spíchal, Z. Pěkná, O. Šamajová, K. Doležal, O. Plíhal, E. Benková, M. Strnad, L. Plíhalová, Design, synthesis and perception of fluorescently labeled isoprenoid cytokinins, Phytochemistry 150 (2018) 1–11, https://doi.org/10.1016/j.phytochem.2018.02.015.

[8] Z. Rajnai, D. Méhn, E. Beéry, A. Okyar, M. Jani, G.K. Tóth, F. Fülöp, F. Lévi, P. Krajcsi, ATP-binding cassette B1 transports seliciclib (R-roscovitine), a cyclin-dependent kinase inhibitor, Drug Metabol. Dispos. 38 (11) (2010) 2000–2006, https://doi.org/10.1124/dmd.110.032805.

[9] A. González-Duarte, M. Cotrina-Vidal, H. Kaufmann, L. Norcliffe-Kaufmann, Familial dysautonomia, Clin. Auton. Res. 33 (3) (2023) 269–280, https://doi.org/10.1007/s10286-023-00941-1.

[10] M. Hönig, L. Plíhalová, L. Spíchal, J. Grúz, A. Kadlecová, J. Voller, A.R. Svobodová, J. Vostálová, J. Ulrichová, K. Doležal, M. Strnad, New cytokinin derivatives possess UVA and UVB photoprotective effect on human skin cells and prevent oxidative stress, Eur. J. Med. Chem. 150 (2018) 946–957, https://doi.org/10.1016/j.ejmech.2018.03.043.

[11] M. Pertea, G.M. Pertea, C.M. Antonescu, T.C. Chang, J.T. Mendell, S.L. Salzberg, StringTie enables improved reconstruction of a transcriptome from RNA-seq reads, Nat. Biotechnol. 33 (3) (2015) 290–295, https://doi.org/10.1038/nbt.3122.

[12] M. Martin, Cutadapt removes adapter sequences from high-throughput sequencing reads, EMBnet. journal 17 (1) (2011) 10–12, https://doi.org/10.14806/ej.17.1.200.

[13] A. Dobin, C.A. Davis, F. Schlesinger, J. Drenkow, C. Zaleski, S. Jha, P. Batut, M. Chaisson, T.R. Gingeras, STAR: ultrafast universal RNA-seq aligner, Bioinformatics 29 (1) (2013) 15–21, https://doi.org/10.1093/bioinformatics/bts635.

[14] R. Patro, G. Duggal, M.I. Love, R.A. Irizarry, C. Kingsford, Salmon provides fast and bias-aware quantification of transcript expression, Nat. Methods 14 (4) (2017) 417–419, https://doi.org/10.1038/nmeth.4197.

[15] G. Yu, L.G. Wang, Y. Han, Q.Y. He, clusterProfiler: an R package for comparing biological themes among gene clusters, OMICS A J. Integr. Biol. 16 (5) (2012) 284–287, https://doi.org/10.1089/omi.2011.0118.

[16] M. Carlson, org.Hs.eg.db: genome wide annotation for Human, R package version 3.8.2 (2019).

[17] L. Zahajská, J. Nisler, J. Voller, T. Gucký, T. Pospíšil, L. Spíchal, M. Strnad, Preparation, characterization and biological activity of C8-substituted cytokinins, Phytochemistry 135 (2017), https://doi.org/10.1016/j.phytochem.2016.12.005.

[18] V. Mik, L. Szüčová, M. Šmehilová, M. Zatloukal, K. Doležal, J. Nisler, J. Grúz, P. Galuszka, M. Strnad, L. Spíchal, N9-substituted derivatives of kinetin: effective anti-senescence agents, Phytochemistry 72 (8) (2011) 821–831, https://doi.org/10.1016/j.phytochem.2011.02.002.

[19] J. Walla, L. Szüčová, I. Císařová, T. Gucký, M. Zatloukal, K. Doležal, J. Greplová, F. J. Massino, M. Strnad, X-ray structure, NMR and stability-in-solution study of 6-(furfurylamino)-9-(tetrahydropyran-2-yl)purine - a new active compound for cosmetology, J. Mol. Struct. 975 (1–3) (2010) 376–380, https://doi.org/10.1016/j.molstruc.2010.05.013.

[20] S.L. Anderson, R. Coli, I.W. Daly, E.A. Kichula, M.J. Rork, S.A. Volpi, J. Ekstein, B. Y. Rubin, Familial dysautonomia is caused by mutations of the IKAP gene, Am. J. Hum. Genet. 68 (3) (2001) 753–758, https://doi.org/10.1086/318808.

[21] S.L. Anderson, B. Liu, J. Qiu, A.J. Sturm, J.A. Schwartz, A.J. Peters, K.A. Sullivan, B.Y. Rubin, Nutraceutical-mediated restoration of wild-type levels of IKBKAP-encoded IKAP protein in familial dysautonomia-derived cells, Mol. Nutr. Food Res. 56 (2012) 570–579, https://doi.org/10.1002/mnfr.201100670.

[22] S.L. Anderson, J. Qiu, B.Y. Rubin, Tocotrienols induce IKBKAP expression: a possible therapy for familial dysautonomia, Biochem. Biophys. Res. Commun. 306 (1) (2003) 303–309, https://doi.org/10.1016/S0006-291X(03)00971-9.

[23] S.L. Anderson, J. Qiu, B.Y. Rubin, EGCG corrects aberrant splicing of IKAP mRNA in cells from patients with familial dysautonomia, Biochem. Biophys. Res. Commun. 310 (2) (2003) 627–633, https://doi.org/10.1016/j.bbrc.2003.09.019.

[24] P. Artursson, K. Palm, K. Luthman, Caco-2 monolayers in experimental and theoretical predictions of drug transport, Adv. Drug Deliv. Rev. 46 (1–3) (2001) 27–43, https://doi.org/10.1016/S0169-409X(00)00128-9.

[25] F.B. Axelrod, H. Kaufmann, Familial dysautonomia, in: Encyclopedia of the Neurological Sciences, Elsevier Inc, 2014, pp. 271–274, https://doi.org/10.1016/B978-0-12-385157-4.01038-1.

[26] Felicia B. Axelrod, Familial dysautonomia and other congenital sensory and autonomic neuropathies, in: Cellular and Molecular Biology of Neuronal Development, Springer US, 1984, pp. 331–340, https://doi.org/10.1007/978-1-4613-2717-2_21.

[27] Felicia B. Axelrod, Familial dysautonomia, Muscle Nerve 29 (3) (2004) 352–363, https://doi.org/10.1002/mus.10499.

[28] Felicia B. Axelrod, J.D. Goldberg, X.Y. Ye, C. Maayan, Survival in familial dysautonomia: impact of early intervention, J. Pediatr. 141 (4) (2002) 518–523, https://doi.org/10.1067/mpd.2002.127088.

[29] Felicia B. Axelrod, L. Liebes, G. G. Von Simson, S. Mendoza, J. Mull, M. Leyne, L. Norcliffe-Kaufmann, H. Kaufmann, S.A. Slaugenhaupt, Kinetin improves IKBKAP mRNA splicing in patients with familial dysautonomia, Pediatr. Res. 70 (5) (2011) 480–483, https://doi.org/10.1203/PDR.0b013e31822e1825.

[30] R. Bochner, Y. Ziv, D. Zeevi, M. Donyo, L. Abraham, R. Ashery-Padan, G. Ast, Phosphatidylserine increases IKBKAP levels in a humanized knock-in IKBKAP mouse model, Hum. Mol. Genet. 22 (14) (2013) 2785–2794, https://doi.org/10.1093/hmg/ddt126.

[31] F. Bonnier, M.E. Keating, T.P. Wróbel, K. Majzner, M. Baranska, A. Garcia-Munoz, A. Blanco, H.J. Byrne, Cell viability assessment using the Alamar blue assay: a comparison of 2D and 3D cell culture models, Toxicol. Vitro 29 (1) (2015) 124–131, https://doi.org/10.1016/j.tiv.2014.09.014.

[33] L.E. Bowie, T. Maiuri, M. Alpaugh, M. Gabriel, N. Arbez, D. Galleguillos, C.L. K. Hung, S. Patel, J. Xia, N.T. Hertz, C.A. Ross, D.W. Litchfield, S. Sipione, R. Truant, $N^6$-Furfuryladenine is protective in Huntington's disease models by signaling huntingtin phosphorylation, Proc. Natl. Acad. Sci. USA 115 (30) (2018) E7081–E7090, https://doi.org/10.1073/pnas.1801772115.

[34] S.R. Breshears, S.S. Wang, S.G. Bechtolt, B.E. Christensen, Purines. VIII. The aminolysis of certain chlorosubstituted purines [1], J. Am. Chem. Soc. 81 (14) (1959) 3789–3792, https://doi.org/10.1021/ja01523a075.

[36] M. Chaverra, L. George, M. Mergy, H. Waller, K. Kujawa, C. Murnion, E. Sharples, J. Thorne, N. Podgajny, A. Grindeland, Y. Ueki, S. Eiger, C. Cusick, A. Michael Babcock, G.A. Carlson, F. Lefcort, The familial dysautonomia disease gene IKBKAP is required in the developing and adult mouse central nervous system, DMM Disease Models and Mechanisms 10 (5) (2017) 605–618, https://doi.org/10.1242/dmm.028258.

[37] D. Cheishvili, C. Maayan, Y. Smith, G. Ast, A. Razin, IKAP/hELP1 deficiency in the cerebrum of familial dysautonomia patients results in down regulation of genes involved in oligodendrocyte differentiation and in myelination, Hum. Mol. Genet. 16 (17) (2007) 2097–2104, https://doi.org/10.1093/hmg/ddm157.

[38] P. Close, N. Hawkes, I. Cornez, C. Creppe, C.A. Lambert, B. Rogister, U. Siebenlist, M.P. Merville, S.A. Slaugenhaupt, V. Bours, J.Q. Svejstrup, A. Chariot, Transcription impairment and cell migration defects in elongator-depleted cells: implication for familial dysautonomia, Mol. Cell 22 (4) (2006) 521–531, https://doi.org/10.1016/j.molcel.2006.04.017.

[40] C. Creppe, L. Malinouskaya, M.L. Volvert, M. Gillard, P. Close, O. Malaise, S. Laguesse, I. Cornez, S. Rahmouni, S. Ormenese, S. Belachew, B. Malgrange, J. P. Chapelle, U. Siebenlist, G. Moonen, A. Chariot, L. Nguyen, Elongator controls the migration and differentiation of cortical neurons through acetylation of α-tubulin, Cell 136 (3) (2009) 551–564, https://doi.org/10.1016/j.cell.2008.11.043.

[41] M.P. Cuajungco, M. Leyne, J. Mull, S.P. Gill, W. Lu, D. Zagzag, F.B. Axelrod, C. Maayan, J.F. Gusella, S.A. Slaugenhaupt, Tissue-specific reduction in splicing efficiency of IKBKAP due to the major mutation associated with familial dysautonomia, Am. J. Hum. Genet. 72 (3) (2003) 749–758, https://doi.org/10.1086/368263.

[42] A. Daina, V. Zoete, A BOILED-egg to predict gastrointestinal absorption and brain penetration of small molecules, ChemMedChem 11 (11) (2016) 1117–1121, https://doi.org/10.1002/cmdc.201600182.

[43] L. Di, E.H. Kerns, Profiling drug-like properties in discovery research, Curr. Opin. Chem. Biol. 7 (3) (2003) 402–408, https://doi.org/10.1016/S1367-5931(03)00055-3. Elsevier Ltd.

[44] I. Donadon, M. Pinotti, K. Rajkowska, G. Pianigiani, E. Barbon, E. Morini, H. Motaln, B. Rogelj, F. Mingozzi, S.A. Slaugenhaupt, F. Pagani, Exon-specific U1 snRNAs improve ELP1 exon 20 definition and rescue ELP1 protein expression in a familial dysautonomia mouse model, Hum. Mol. Genet. 27 (14) (2018) 2466–2476, https://doi.org/10.1093/hmg/ddy151.

[46] N.A. Hawkes, G. Otero, G. Sebastiaan Winkler, N. Marshall, M.E. Dahmus, D. Krappmann, C. Scheidereit, C.L. Thomas, G. Schiavo, H. Erdjument-Bromage, J. Q. Svejstrup, Purification and characterization of the human elongator complex, J. Biol. Chem. 277 (4) (2002) 3047–3052, https://doi.org/10.1074/jbc.M110445200.

[47] N.T. Hertz, A. Berthet, M.L. Sos, K.S. Thorn, A.L. Burlingame, K. Nakamura, K. M. Shokat, A neo-substrate that amplifies catalytic activity of Parkinson's-disease-related kinase PINK1, Cell 154 (4) (2013) 737–747, https://doi.org/10.1016/j.cell.2013.07.030.

[48] M. Hervé, E.C. Ibrahim, Proteasome inhibitors to alleviate aberrant IKBKAP mRNA splicing and low IKAP/hELP1 synthesis in familial dysautonomia, Neurobiol. Dis. 103 (2017) 113–122, https://doi.org/10.1016/j.nbd.2017.04.009.

[49] M.J. Hilz, Assessing function and pathology in familial dysautonomia: assessment of temperature perception, sweating and cutaneous innervation, Brain 127 (9) (2004) 2090–2098, https://doi.org/10.1093/brain/awh235.

[50] M.M. Hims, R.S. Shetty, J. Pickel, J. Mull, M. Leyne, L. Liu, J.F. Gusella, S. A. Slaugenhaupt, A humanized IKBKAP transgenic mouse models a tissue-specific human splicing defect, Genomics 90 (3) (2007) 389–396, https://doi.org/10.1016/j.ygeno.2007.05.012.

[52] M. Huang, Y. Wang, S.B. Cogut, B.S. Mitchell, L.M. Graves, Inhibition of nucleoside transport by protein kinase inhibitors, J. Pharmacol. Exp. Therapeut. 304 (2) (2003) 753–760, https://doi.org/10.1124/jpet.102.044214.

[53] J.D. Irvine, L. Takahashi, K. Lockhart, J. Cheong, J.W. Tolan, H.E. Selick, J. R. Grove, MDCK (Madin-Darby canine kidney) cells: a tool for membrane permeability screening, J. Pharmaceut. Sci. 88 (1) (1999) 28–33, https://doi.org/10.1021/js9803205.

[54] L.D. Johansen, T. Naumanen, A. Knudsen, N. Westerlund, I. Gromova, M. Junttila, C. Nielsen, T. Bøttzauw, A. Tolkovsky, J. Westermarck, E.T. Coffey, M. Jäättelä, T. Kallunki, IKAP localizes to membrane ruffles with filamin A and regulates actin cytoskeleton organization and cell migration, J. Cell Sci. 121 (6) (2008) 854–864, https://doi.org/10.1242/jcs.013722.

[55] A. Kadlecová, B. Maková, M. Artal-Sanz, M. Strnad, J. Voller, The plant hormone kinetin in disease therapy and healthy aging, in: Ageing Research Reviews, vol. 55, Elsevier Ireland Ltd, 2019, https://doi.org/10.1016/j.arr.2019.100958.

[56] H. Keren, M. Donyo, D. Zeevi, C. Maayan, T. Pupko, G. Ast, Phosphatidylserine increases IKBKAP levels in familial dysautonomia cells, PLoS One 5 (12) (2010) e15884, https://doi.org/10.1371/journal.pone.0015884.

[57] J.H. Kim, W.S. Lane, D. Reinberg, Human elongator facilitates RNA polymerase II transcription through chromatin, Proc. Natl. Acad. Sci. U.S.A. 99 (3) (2002) 1241–1246, https://doi.org/10.1073/pnas.251672198.

[58] F. Konietschke, O. Libiger, L.A. Hothorn, Nonparametric evaluation of quantitative traits in population-based association studies when the genetic model is unknown, PLoS One 7 (2) (2012), https://doi.org/10.1371/journal.pone.0031242.

[59] J. Kumar Singh, A. Solanki, Rapid equilibrium dialysis (RED): an in-vitro high-throughput screening technique for plasma protein binding using human and rat plasma, J. Bioequivalence Bioavailab. s14 (2012), https://doi.org/10.4172/jbb.s14-005.

[60] G. Lee, E.P. Papapetrou, H. Kim, S.M. Chambers, M.J. Tomishima, C.A. Fasano, Y. M. Ganat, J. Menon, F. Shimizu, A. Viale, V. Tabar, M. Sadelain, L. Studer, Modelling pathogenesis and treatment of familial dysautonomia using patient-specific iPSCs, Nature 461 (7262) (2009) 402–406, https://doi.org/10.1038/nature08320.

[61] G. Lee, C.N. Ramirez, H. Kim, N. Zeltner, B. Liu, C. Radu, B. Bhinder, Y.J. Kim, I. Y. Choi, B. Mukherjee-Clavin, H. Djaballah, L. Studer, Large-scale screening using familial dysautonomia induced pluripotent stem cells identifies compounds that rescue IKBKAP expression, Nat. Biotechnol. 30 (12) (2012) 1244–1248, https://doi.org/10.1038/nbt.2435.

[62] S. Lefler, M.A. Cohen, G. Kantor, D. Cheishvili, A. Even, A. Birger, T. Turetsky, Y. Gil, S. Even-Ram, E. Aizenman, N. Bashir, C. Maayan, A. Razin, B.E. Reubinoff, M. Weil, Familial dysautonomia (FD) human embryonic stem cell derived PNS neurons reveal that synaptic vesicular and neuronal transport genes are directly or indirectly affected by IKBKAP downregulation, PLoS One 10 (10) (2015) e0138807, https://doi.org/10.1371/journal.pone.0138807.

[63] B. Liu, S.L. Anderson, J. Qiu, B.Y. Rubin, Cardiac glycosides correct aberrant splicing of *IKBKAP* -encoded mRNA in familial dysautonomia derived cells by suppressing expression of SRSF3, FEBS J. 280 (15) (2013) 3632–3646, https://doi.org/10.1111/febs.12355.

[64] Y.-S. Liu, C. Zhao, D.E. Bergbreiter, D. Romo, Simultaneous deprotection and purification of BOC-amines based on ionic resin capture, J. Org. Chem. 63 (10) (1998) 3471–3473, https://doi.org/10.1021/jo972001o.

[65] V. Mik, Z. Mičková, K. Doležal, I. Frébort, T. Pospíšil, Activity of (+)-Discadenine as a plant cytokinin, J. Nat. Prod. 80 (7) (2017) 2136–2140, https://doi.org/10.1021/acs.jnatprod.6b01165.

[66] E. Morini, P. Dietrich, M. Salani, H.M. Downs, G.R. Wojtkiewicz, S. Alli, A. Brenner, M. Nilbratt, J.W. LeClair, A.L. Oaklander, S.A. Slaugenhaupt, I. Dragatsis, Sensory and autonomic deficits in a new humanized mouse model of familial dysautonomia, Hum. Mol. Genet. 25 (6) (2016) 1116–1128, https://doi.org/10.1093/hmg/ddv634.

[67] E. Morini, D. Gao, E.M. Logan, M. Salani, A.J. Krauson, A. Chekuri, S. A. Slaugenhaupt, Developmental regulation of neuronal gene expression by Elongator complex protein 1 dosage, Journal of Genetics and Genomics 49 (7) (2022) 654–665, https://doi.org/10.1016/j.jgg.2021.11.011.

[68] S. Naftelberg, Z. Abramovitch, S. Gluska, S. Yannai, Y. Joshi, M. Donyo, K. Ben-Yaakov, T. Gradus, J. Zonszain, C. Farhy, R. Ashery-Padan, E. Perlson, G. Ast, Phosphatidylserine ameliorates neurodegenerative symptoms and enhances axonal transport in a mouse model of familial dysautonomia, PLoS Genet. 12 (12) (2016) e1006486, https://doi.org/10.1371/journal.pgen.1006486.

[70] J.A. Palma, L. Norcliffe-Kaufmann, C. Fuente-Mora, L. Percival, C. Mendoza-Santiesteban, H. Kaufmann, Current treatments in familial dysautonomia, Expet Opin. Pharmacother. 15 (18) (2014) 2653–2671, https://doi.org/10.1517/14656566.2014.970530. Informa Healthcare.

[72] P.B. Rahl, C.Z. Chen, R.N. Collins, Elp1p, the yeast homolog of the FD disease syndrome protein, negatively regulates exocytosis independently of transcriptional elongation, Mol. Cell 17 (6) (2005) 841–853, https://doi.org/10.1016/j.molcel.2005.02.018.

[73] C.M. Riley, R.L. Day, D.M. Greeley, W.S. Langford, Central autonomic dysfunction with defective lacrimation; report of five cases, Pediatrics 3 (4) (1949) 468–478.

[74] B.Y. Rubin, S.L. Anderson, IKBKAP/ELP1 gene mutations: mechanisms of familial dysautonomia and gene-targeting therapies, Appl. Clin. Genet. 10 (2017) 95–103, https://doi.org/10.2147/TACG.S129638. Dove Medical Press Ltd.

[75] M. Salani, F. Urbina, A. Brenner, E. Morini, R. Shetty, C.S. Gallagher, E.A. Law, S. Sunshine, D.J. Finneran, G. Johnson, L. Minor, S.A. Slaugenhaupt, Development of a screening platform to identify small molecules that modify ELP1 pre-mRNA splicing in familial dysautonomia, SLAS Discovery : Advancing Life Sciences R & D 24 (1) (2019) 57–67, https://doi.org/10.1177/2472555218792264.

[76] Y. Sambuy, I. De Angelis, G. Ranaldi, M.L. Scarino, A. Stammati, F. Zucco, The Caco-2 cell line as a model of the intestinal barrier: influence of cell and culture-related factors on Caco-2 cell functional characteristics, Cell Biol. Toxicol. 21 (1) (2005) 1–26, https://doi.org/10.1007/s10565-005-0085-6.

[77] M. Shohat, M. Weisz Hubshman, Familial Dysautonomia. *GeneReviews* (R), University of Washington, Seattle, WA, 1993.

[79] R. Sinha, Y.J. Kim, T. Nomakuchi, K. Sahashi, Y. Hua, F. Rigo, C.F. Bennett, A. R. Krainer, Antisense oligonucleotides correct the familial dysautonomia splicing defect in IKBKAP transgenic mice, Nucleic Acids Res. 46 (10) (2018) 4833–4844, https://doi.org/10.1093/nar/gky249.

[80] S.A. Slaugenhaupt, A. Blumenfeld, S.P. Gill, M. Leyne, J. Mull, M.P. Cuajungco, C. B. Liebert, B. Chadwick, M. Idelson, L. Reznik, C.M. Robbins, I. Makalowska, M. J. Brownstein, S.A. Slaugenhaupt, C. Scheidereit, C. Maayan, F.B. Axelrod, J. F. Gusella, Tissue-specific expression of a splicing mutation in the IKBKAP gene causes familial dysautonomia, Am. J. Hum. Genet. 68 (3) (2001) 598–605, https://doi.org/10.1086/318810.

[81] S.A. Slaugenhaupt, J. Mull, M. Leyne, M.P. Cuajungco, S.P. Gill, M.M. Hims, F. Quintero, F.B. Axelrod, J.F. Gusella, Rescue of a human mRNA splicing defect by the plant cytokinin kinetin, Hum. Mol. Genet. 13 (4) (2004) 429–436, https://doi.org/10.1093/hmg/ddh046.

[82] A. Smith, A. Farbman, J. Dancis, Absence of taste-bud papillae in familial dysautonomia, Science 147 (3661) (1965) 1040–1041, https://doi.org/10.1126/science.147.3661.1040.

[84] E.Y. Sutcliffe, R.K. Robins, Electron density and orientation of nucleophilic substitution in the purine ring [1], J. Org. Chem. 28 (6) (1963) 1662–1666, https://doi.org/10.1021/jo01041a057.

[85] D. Taddei, P. Kilian, A.M.Z. Slawin, J.D. Woollins, Synthesis and full characterisation of 6-chloro-2-iodopurine, a template for the functionalisation of purines, Org. Biomol. Chem. 2 (5) (2004) 665–670, https://doi.org/10.1039/b312629c.

[86] M. Valensi-Kurtz, S. Lefler, M.A. Cohen, M. Aharonowiz, R. Cohen-Kupiec, A. Sheinin, U. Ashery, B. Reubinoff, M. Weil, Enriched population of PNS neurons derived from human embryonic stem cells as a platform for studying peripheral neuropathies, PLoS One 5 (2) (2010) e9290, https://doi.org/10.1371/journal.pone.0009290.

[87] J. Voller, B. Maková, A. Kadlecová, G. Gonzalez, M. Strnad, Plant hormone cytokinins for modulating human aging and age-related diseases, Hormones in ageing and longevity (2017) 311–335, https://doi.org/10.1007/978-3-319-63001-4_14.

[88] Q. Wang, J.D. Rager, K. Weinstein, P.S. Kardos, G.L. Dobson, J. Li, I.J. Hidalgo, Evaluation of the MDR-MDCK cell line as a permeability screen for the blood-brain barrier, Int. J. Pharm. 288 (2) (2005) 349–359, https://doi.org/10.1016/j.ijpharm.2004.10.007.

[89] J. Wu, Statistical inference for tumor growth inhibition T/C ratio, J. Biopharm. Stat. 20 (5) (2010) 954–964, https://doi.org/10.1080/10543401003618983.

[90] X. Wu, J. Wang, L. Tan, J. Bui, E. Gjerstad, K. McMillan, W. Zhang, In vitro ADME profiling using high-throughput RapidFire mass spectrometry, J. Biomol. Screen 17 (6) (2012) 761–772, https://doi.org/10.1177/1087057112441013.

[91] M. Yoshida, N. Kataoka, K. Miyauchi, K. Ohe, K. Iida, S. Yoshida, T. Nojima, Y. Okuno, H. Onogi, T. Usui, A. Takeuchi, T. Hosoya, T. Suzuki, M. Hagiwara, Rectifier of aberrant mRNA splicing recovers tRNA modification in familial dysautonomia, Proc. Natl. Acad. Sci. U.S.A. 112 (9) (2015) 2764–2769, https://doi.org/10.1073/pnas.1415525112.

[92] H. Yu, Q. Wang, Y. Sun, M. Shen, H. Li, Y. Duan, A new PAMPA model proposed on the basis of a synthetic phospholipid membrane, PLoS One 10 (2) (2015) e0116502, https://doi.org/10.1371/journal.pone.0116502.

[93] N. Zeltner, F. Fattahi, N.C. Dubois, N. Saurat, F. Lafaille, L. Shang, B. Zimmer, J. Tchieu, M.A. Soliman, G. Lee, J.L. Casanova, L. Studer, Capturing the biology of disease severity in a PSC-based model of familial dysautonomia, Nat. Med. 22 (12) (2016) 1421–1427, https://doi.org/10.1038/nm.4220.

[94] D. Zhang, G. Luo, X. Ding, C. Lu, Preclinical experimental models of drug metabolism and disposition in drug discovery and development, Acta Pharm. Sin. B 2 (6) (2012) 549–561, https://doi.org/10.1016/j.apsb.2012.10.004.

[95] W. Ried, H. Woithe, A. Müller, Strukturaufklärung von $N^6$ -, 9- und 7-Acyladeninen durch $^1$H-und $^{13}$C-NMR-Spektroskopie von Festkörpern und in Lösung, Helv. Chim. Acta 72 (7) (1989) 1597–1607, https://doi.org/10.1002/hlca.19890720720.

[99] N. Boone, A. Bergon, B. Loriod, A. Devèze, C. Nguyen, F.B. Axelrod, E.C. Ibrahim, Genome-wide analysis of familial dysautonomia and kinetin target genes with patient olfactory ecto-mesenchymal stem cells, Hum. Mutat. 33 (3) (2012) 530–540. https://doi.org/10.1002/humu.22010.

[101] M. Pertea, G.M. Pertea, C.M. Antonescu, T.C. Chang, J.T. Mendell, S.L. Salzberg, StringTie enables improved reconstruction of a transcriptome from RNA-seq reads, Nat. Biotechnol. 33 (3) (2015) 290–295. https://doi.org/10.1038/nbt.3122.

[102] H. Pimentel, N.L. Bray, S. Puente, P. Melsted, L. Pachter, Differential analysis of RNA-seq incorporating quantification uncertainty, Nat. Methods 14 (7) (2017) 687–690. https://doi.org/10.1038/nmeth.4324.

[103] M. Carlson, GO.db: A set of annotation maps describing the entire Gene Ontology, R package version 3.8.2, 2019.

## Further reading


[32] N. Boone, A. Bergon, B. Loriod, A. Devèze, C. Nguyen, F.B. Axelrod, E.C. Ibrahim, Genome-wide analysis of familial dysautonomia and kinetin target genes with patient olfactory ecto-mesenchymal stem cells, Hum. Mutat. 33 (3) (2012) 530–540, https://doi.org/10.1002/humu.22010.

[35] M. Carlson, GO.db: a set of annotation maps describing the entire Gene Ontology, R package version 3.8.2 (2019).

[39] J.S. Cohen, S. Srivastava, K.D. Farwell, H.M. Lu, W. Zeng, H. Lu, E.C. Chao, A. Fatemi, ELP2 is a novel gene implicated in neurodevelopmental disabilities, Am. J. Med. Genet. 167 (6) (2015) 1391–1395, https://doi.org/10.1002/ajmg.a.36935.

[45] Familial Dysautonomia - GeneReviews® - NCBI Bookshelf. (n.d.). Retrieved January 16, 2020, from https://www.ncbi.nlm.nih.gov/books/NBK1180/.

[51] C. Holmberg, S. Katz, M. Lerdrup, T. Herdegen, M. Jäättelä, A. Aronheim, T. Kallunki, A novel specific role for IκB kinase complex-associated protein in cytosolic stress signaling, J. Biol. Chem. 277 (35) (2002) 31918–31928, https://doi.org/10.1074/jbc.M200719200.

[69] H. Najmabadi, H. Hu, M. Garshasbi, T. Zemojtel, S.S. Abedini, W. Chen, M. Hosseini, F. Behjati, S. Haas, P. Jamali, A. Zecha, M. Mohseni, L. Püttmann, L. N. Vahid, C. Jensen, L.A. Moheb, M. Bienek, F. Larti, I. Mueller, H.H. Ropers, Deep sequencing reveals 50 novel genes for recessive cognitive disorders, Nature 478 (7367) (2011) 57–63, https://doi.org/10.1038/nature10423.

[71] H. Pimentel, N.L. Bray, S. Puente, P. Melsted, L. Pachter, Differential analysis of RNA-seq incorporating quantification uncertainty, Nat. Methods 14 (7) (2017) 687–690, https://doi.org/10.1038/nmeth.4324.

[78] C.L. Simpson, R. Lemmens, K. Miskiewicz, W.J. Broom, V.K. Hansen, P.W.J. van Vught, J.E. Landers, P. Sapp, L. Van Den Bosch, J. Knight, B.M. Neale, M.R. Turner, J.H. Veldink, R.A. Ophoff, V.B. Tripathi, A. Beleza, M.N. Shah, P. Proitsi, A. Van Hoecke, A. Al-Chalabi, Variants of the elongator protein 3 (ELP3) gene are associated with motor neuron degeneration, Hum. Mol. Genet. 18 (3) (2009) 472–481, https://doi.org/10.1093/hmg/ddn375.

[83] L.J. Strug, T. Clarke, T. Chiang, M. Chien, Z. Baskurt, W. Li, R. Dorfman, B. Bali, E. Wirrell, S.L. Kugler, D.E. Mandelbaum, S.M. Wolf, P. McGoldrick, H. Hardison, E.J. Novotny, J. Ju, D.A. Greenberg, J.J. Russo, D.K. Pal, Centrotemporal sharp wave EEG trait in rolandic epilepsy maps to Elongator Protein Complex 4 (ELP4), Eur. J. Hum. Genet. 17 (9) (2009) 1171–1181, https://doi.org/10.1038/ejhg.2008.267.